Article

Not peer-reviewed version

Techno-Economic and Carbon Payback Assessment of an ICE-to-EV Institutional Shuttle Fleet with Distributed PV–BESS Charging Sized via Closed-Form KKT Active-Constraint Analysis

Kittinun Srasuay , Nopporn Patcharaprakiti , Jutturit Thongpron , Anon Namin , Montri Ngao-det , Naris Khampangkaew , Nattawat Panlawan , Kan Nakaiam , Worrajak Muangjai , Teerasak Somsak *

Posted Date: 12 May 2026

doi: 10.20944/preprints202605.0703.v1

Keywords: electric shuttle fleet; distributed PV–BESS charging station; KKT active-constraint analysis; closed-form sizing rule; techno-economic assessment; stochastic NPV analysis; carbon payback period; institutional fleet electrification

 doi:10.20944/preprints202605.0703.v1

Article

Techno-Economic and Carbon Payback Assessment of an ICE-to-EV Institutional Shuttle Fleet with Distributed PV–BESS Charging Sized via Closed-Form KKT Active-Constraint Analysis

Kittinun Srasuay, Nopporn Patcharaprakiti, Jutturit Thongpron, Anon Namin, Montri Ngao-det, Naris Khampangkaew, Nattawat Panlawan, Kan Nakaiam, Worrajak Muangjai and Teerasak Somsak *

Clean Energy System Research Unit (CES-RMUTL), Division of Electrical Engineering, Faculty of Engineering, Rajamangala University of Technology Lanna (RMUTL), Chiang Mai 50300, Thailand

* Correspondence: dhirasak@rmutl.ac.th

Abstract

Institutional shuttle fleets with fixed routes and predictable terminal parking are well suited to dedicated photovoltaic–battery (PV–BESS) charging infrastructure, yet siting and sizing are usually solved numerically without clear interpretation of the governing constraints. This study develops a closed-form active-constraint sizing rule, derived via Karush–Kuhn–Tucker (KKT) analysis under verified monotonicity of the net-present-value (NPV) objective over the feasible design region, for a 10-van electric academic shuttle fleet operating between the Huay Kaew and Doi Saket campuses of Rajamangala University of Technology Lanna, Chiang Mai, Thailand. One centralized station is compared with two distributed stations under reliability, cost, solar-fraction, autonomy, charger, budget, and rooftop-area constraints. The two-station configuration eliminates 47,600 km/year of dead-run travel and increases system NPV from USD 36,980 to USD 86,293 after the year-10 BESS replacement cost. The KKT analysis identifies two binding constraints—BESS one-day autonomy and PV rooftop area—giving 30 kWp PV and 94.85 kWh BESS per station, rounded to 100 kWh. The full transition achieves IRR = 12.9%, simple payback = 6.1 years, and 95.9% annual CO_2 reduction. Monte Carlo simulation with 5,000 scenarios yields $P(NPV > 0) = 100\%$ within the simulated scenario set, $VaR_{5\%} = USD\ 28{,}959$, and $CVaR_{5\%} = USD\ 21{,}248$, confirming financial robustness under the adopted uncertainty ranges.

Keywords: electric shuttle fleet; distributed PV–BESS charging station; KKT active-constraint analysis; closed-form sizing rule; techno-economic assessment; stochastic NPV analysis; carbon payback period; institutional fleet electrification

1. Introduction

The worldwide transportation industry is one of the slowest to decarbonize, accounting for 16% of total greenhouse gas (GHG) emissions, with road transport accounting for around 12% [1,2]. Electric vehicle (EV) adoption is accelerating, with approximately 14 million units delivered in 2023 and expected to exceed 17 million in 2024, with major economies aiming for 30-60% market share by 2030 [1]. However, public charging infrastructure roll-out is still lagging behind fleet expansion. This bottleneck is particularly pronounced in Southeast Asia since land availability, grid capacity and funding processes are very different from the European and North American baselines that currently dominate the study. Within this context, captive institutional vehicle fleets—operated by universities, hospitals, and government agencies—present a distinct and highly advantageous electrification target [3]. Because these fleets follow predictable fixed routes, park centrally overnight, and maintain auditable fuel records, they can safely bypass public-charging limitations by collocating generation,

 doi:10.20944/preprints202605.0703.v1

storage, and charging infrastructure on owned land, making dedicated on-site facilities both technically and economically tractable.

In Thailand, the second-phase BEV incentive scheme, commonly referred to as EV 3.5, has been implemented for 2024–2027 to support electric-vehicle adoption through revised purchase subsidies, excise-tax incentives, and local-production requirements [4]. In this study, EV 3.5 is treated as a supportive policy context rather than a direct cash-flow subsidy, because the eligibility of institutional electric shuttle vans depends on vehicle category, procurement conditions, battery capacity, and the incentive rules in force at the time of purchase. This creates a time-bounded economic window that strongly motivates near-term institutional procurement decisions. Currently, Thailand's grid emission factor stands at 0.4999 $kgCO_2/kWh$ (Thailand Greenhouse Gas Management Organization, TGO, 2024 [5]), implying that even fully grid-charged EVs deliver substantial carbon abatement relative to conventional diesel vehicles. However, when integrated with on-site photovoltaic (PV) generation, the operational emission factor falls below 0.10 $kgCO_2/kWh$, pushing the carbon abatement potential to nearly 95%. Northern Thailand, specifically Chiang Mai (18.81°N, 98.95°E), offers a highly compelling environment for this integration, providing a reliable Peak Solar Hour (PSH) average of 5.02 h/day [6]. This solar resource is entirely sufficient for cost-effective rooftop PV deployment without the need for complex tracking or dual-axis hardware.

The 10-van academic shuttle service of Rajamangala University of Technology Lanna (RMUTL) connects their Huay Kaew (HK) and Doi Saket (DS) campuses on a fixed 28-km route and this service provides a convenient framework for this transition. The vans are permanently assigned to terminals and run on a strict 208-day academic calendar, consisting of 170 normal-semester days and 38 reduced summer-semester days. Unlike the stochastic arrival patterns commonly assumed in the public charging literature, the RMUTL shuttle runs on a highly deterministic charging-demand profile because of the scheduled, terminal-based overnight parking.

Prior techno-economic investigations by the RMUTL Clean Energy System (CES-RMUTL) research group have established a strong foundation in regional renewable energy transitions. Previous studies demonstrated the viability of 100% renewable hybrid PV–hydro–battery microgrids for sustainable rural electrification in Khlong Ruea Thailand, validating HOMER Pro optimization models against field measurements [7], as well as proving the techno-economic feasibility of solar-assisted 48 V mini electric shuttles for carbon-neutral campus operations [8]. The present study extends this analytical tradition from rural off-grid and mini-EV contexts to the dedicated architecture of urban-campus EV fleet charging. Specifically, this paper introduces a closed-form Karush–Kuhn–Tucker (KKT) analytical optimization method for sizing distributed PV–battery energy storage systems (BESS). Furthermore, it explicitly incorporates internal combustion engine (ICE)-to-EV transition economics, carbon payback period assessments, and stochastic Net Present Value (NPV) risk quantification—critical dimensions that remain largely absent from prior regional studies.

Existing techno-economic studies of fleet electrification largely focus on single-station configurations and treat the charging infrastructure as a secondary design element [9–12]. Spatial analyses of public EV charging networks in Thai cities have identified significant service-coverage gaps and sub-optimal siting under current deployment patterns [13]; however, these studies address public-access fast-charging networks [14,15] rather than dedicated captive-fleet infrastructure, which operates under fundamentally different optimization constraints (fixed routes, overnight parking, academic calendar seasonality). Three specific gaps motivate this study:

(1) Academic calendar-aware operating models: Existing fleet electrification studies typically assume year-round continuous operation. No study to date has explicitly quantified how an academic calendar (variable daily trips, 38-day summer reduction, distinct overnight parking locations) reduces annual EV energy demand and reshapes the PV-BESS sizing optimum relative to a 365-day baseline.

 doi:10.20944/preprints202605.0703.v1

(2) Siting optimality: The question of whether one centralized station or multiple distributed stations is economically and operationally optimal has not been formally quantified for dedicated shuttle routes.

(3) Sizing transparency: Existing sizing methods rely on numerical optimization (Genetic Algorithm, Particle Swarm, DE) that converge to a solution without revealing which constraints bind at optimality or why. Establishing whether KKT first-order conditions yield a closed-form result for this class of system would enable rapid engineering design without iterative computation.

Together, these three gaps motivate the present study. Closed-form analytical sizing methods grounded in KKT theory are well established in the convex-optimization literature [16], but their application to PV–BESS charging-station design has been limited by the complexity of public-charging demand patterns. For captive institutional fleets with deterministic demand, the conditions for a closed-form solution are met, and the resulting active-constraint structure provides direct engineering interpretability that metaheuristic methods (Differential Evolution, Genetic Algorithms, Particle Swarm Optimization) cannot supply. Combining this analytical sizing with explicit academic-calendar demand modelling, two-station siting analysis, deterministic techno-economic evaluation, and stochastic NPV risk quantification within a single framework constitutes the methodological contribution of this paper.

Beyond methodology, three substantive parameter gaps in the regional literature also merit attention. First, the economic value attributed to surplus PV electricity in captive-fleet contexts is rarely standardized: studies variably assume feed-in tariffs, internal energy credits, or zero export value, leading to wide variance in reported NPV. Second, the embodied carbon of LFP BESS replacement is frequently omitted from carbon-payback analyses, despite contributing ≈30% of total lifecycle embodied carbon for typical 10–15-year project horizons. Third, downside-risk metrics such as VaR and CVaR are rarely reported for institutional fleet electrification, even though they are the standard risk measures used by public-sector investment committees in Thailand and ASEAN. Addressing these gaps within a single transparent framework is the operational objective of this study.

Closing this gap requires a framework that simultaneously delivers analytical transparency (so that engineers and policy makers can understand which constraints drive sizing decisions), economic realism (so that institutional finance committees can justify capital commitments), and environmental accountability (so that sustainability officers can report verified carbon outcomes). These three requirements are well established in recent reviews of energy-system modelling [18,19] and battery-storage design [17,20], but their joint application to captive institutional EV charging in ASEAN contexts remains an open methodological space.

First, this study develops a closed-form active-constraint sizing rule for distributed PV–BESS charging stations serving a fixed-route institutional electric shuttle fleet, derived via Karush–Kuhn–Tucker (KKT) analysis under verified monotonicity of the NPV objective over the feasible design region. The NPV-maximization problem is formulated with seven technical, operational, and economic constraints, including LOLE reliability, cost competitiveness, minimum solar fraction, BESS autonomy, charger adequacy, budget, and rooftop-area limitation. The KKT analysis shows that the optimum is governed by two active constraints: the BESS one-day autonomy constraint, g_4, and the PV rooftop-area constraint, g_7. This yields explicit sizing rules, $E^{*}_{\mathrm{BESS},i} = \frac{E^{\mathrm{day}}_{\mathrm{EV},i}}{\eta_{\mathrm{BESS}} DOD}$ and $P^{*}_{\mathrm{PV},i} = P^{\max}_{\mathrm{PV}}$. For the revised RMUTL shuttle case, the analytical solution gives 30 kWp PV and 94.85 kWh BESS per station, which is rounded to a practical 100 kWh LFP BESS module. The resulting system-level design is therefore 60 kWp PV and 200 kWh BESS for the two distributed stations.

Second, this study quantifies the siting and academic-calendar effects that are often neglected in institutional fleet-electrification studies. A single centralized station is compared with two distributed terminal-based stations under the actual RMUTL shuttle operating structure. The two-station configuration eliminates 47,600 km/year of non-revenue dead-run travel, avoids 8,901 kWh/year of unnecessary EV energy consumption, and increases system NPV from USD 36,980 to USD 86,293. In addition, the 208-day academic operating calendar is explicitly incorporated into the annual

 doi:10.20944/preprints202605.0703.v1

charging-demand model. This prevents overestimation of annual EV energy demand and clarifies the distinction between annual energy throughput, which affects economic performance and PV surplus, and peak daily demand, which governs BESS autonomy sizing.

Third, this study integrates deterministic optimization with financial, environmental, and stochastic risk assessment in a single planning framework. The deterministic KKT-derived system is evaluated using NPV, IRR, payback period, total cost of ownership, CO_2 reduction, carbon payback period, and Monte Carlo NPV risk metrics. The proposed EV + PV–BESS transition achieves NPV = USD 86,293, IRR = 12.9%, and a simple payback period of 6.1 years under the base-case assumptions. Environmentally, annual CO_2 emissions are reduced from 64.39 tCO_2/year to 2.64 tCO_2/year, corresponding to a 95.9% reduction, while the PV–BESS embodied carbon is recovered within approximately 0.83 years. Monte Carlo simulation with 5,000 scenarios further confirms financial robustness, with $P(NPV > 0) = 100\%$ and $VaR_{5\%}$ = USD 28,959 and $CVaR_{5\%}$ =USD 21,248.

2. Materials and Methods

2.1. Study Site and Route Characterization

The study site is the institutional shuttle route between the Huay Kaew (HK) and Doi Saket (DS) campuses of Rajamangala University of Technology Lanna (RMUTL), Chiang Mai, Thailand (Figure 1). The one-way route distance is approximately 28 km. The existing operation is based on a 10-vehicle diesel van fleet, and the proposed scenario replaces this with 10 electric shuttle vans on the same fixed route. The shuttle operates 208 days per year, following the academic calendar. The fleet is divided evenly into two terminal-based groups: 5 vans permanently assigned to the HK terminal (Group A) and 5 vans permanently assigned to the DS terminal (Group B). Each vehicle completes 3 one-way service trips per day during the normal academic semester: morning (07:00–08:00), midday (12:00–13:00), and evening (16:00–17:00). After the final trip, vehicles return to their home terminal for overnight charging before commencing the next operating day. This terminal-based assignment is fixed throughout the project lifetime and yields a constant nightly charging demand of 78.54 kWh/day at each station during normal-semester operation. Similar institutional inter-campus EV mobility studies have shown that university-operated electric van services with fixed routes and PV-supported charging can provide measurable energy, economic, and CO_2-reduction benefits when schedules, charging access, and operational monitoring are explicitly considered [22].

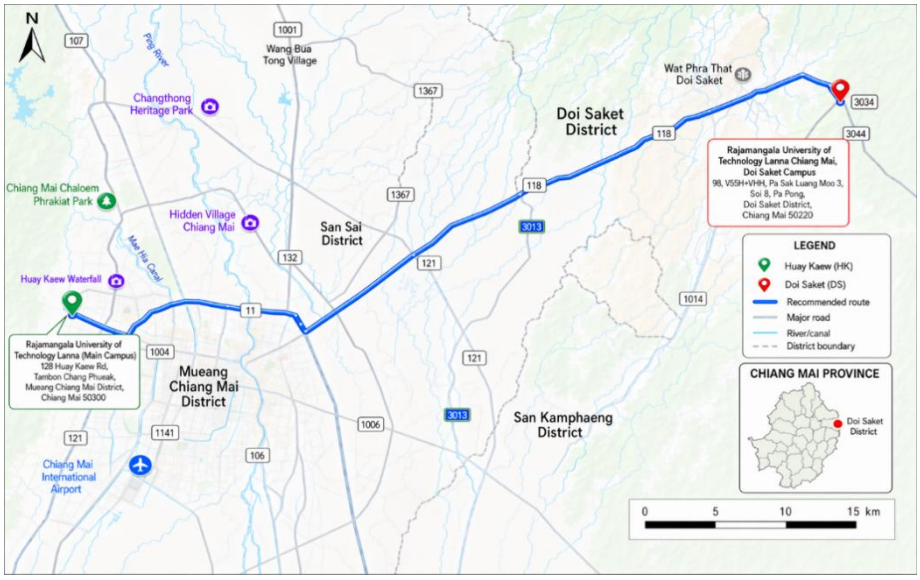

Figure 1. Schematic map of the RMUTL electric academic shuttle route (Map data: ©2026 Google).

 doi:10.20944/preprints202605.0703.v1

The fleet is divided into two operating groups according to the terminal base. Van Group A is based at the Huay Kaew terminal, whereas Van Group B is based at the Doi Saket terminal. Each group consists of five vans, resulting in a total fleet size of 10 vans. During the normal academic semester, both groups operate 15 one-way trips per day. During the reduced summer semester, the HK-based group continues operating at a reduced service level of 10 one-way trips per day, while the DS-based group is assumed to be unavailable for maintenance. The annual operating calendar therefore consists of 170 normal-semester days and 38 reduced summer-semester days for the HK-based group, while the DS-based group operates during the 170 normal-semester days only.

The baseline diesel fuel consumption is estimated using an average fuel efficiency of 7.50 km/L. Based on the annual service distance, the HK-based group travels 82,040 km/year and consumes approximately 10,939 L/year of diesel. The DS-based group travels 71,400 km/year and consumes approximately 9,520 L/year. Thus, the total baseline shuttle operation represents 153,440 km/year and 20,459 L/year of diesel consumption. These values provide the reference case for evaluating the energy demand, fuel cost savings, and CO_2 emission reduction of the proposed electric shuttle van fleet as shown in Table 1.

Table 1. route and fleet characterization for the 10-van diesel baseline and EV replacement scenario.

Parameter	Van A (HK base)	Van B (DS base)	System Total
Fleet size	5 Vans	5 Vans	10 Vans
One-way route distance	28.0 km	28.0 km	-
Travel time (one-way)	40 min	40 min	-
Trips per day (normal semester)	15 one-way trips/day	15 one-way trips/day	30 one-way trips/day
Trips per day (summer, reduced)	10 one-way trips/day	0 (maintenance)	10 one-way trips/day
Annual operating days	208 days, 170 + 38	170 days only	-
Annual distance	82,040 km/year	71,400 km/year	153,440 km/year
Annual diesel	10,939 L/year	9,520 L/year	20,459 L/year
Fuel efficiency (km/L)	7.50 km/L	7.50 km/L	7.50 km/L
Proposed replacement vehicle	Electric shuttle van	Electric shuttle van	Electric shuttle van

2.2. Vehicle Energy Consumption Model

The replacement vehicle is represented by a battery-electric shuttle van using an adopted representative specification: a 90 kWh lithium-ion pack, curb weight of 2,239 kg, NEDC range of 570 km, and operational energy consumption of 0.187 kWh/km (5.3 km/kWh). These parameters are used for route-energy modelling and are summarized in Table 2.

Traction energy demand uses a distance-based linear model [23]:

$$E_{j,t} = d_{\mathrm{ow}} e_{\mathrm{EV}} n_{j,t} \quad (1)$$

where $E_{j,t}$ is the charging energy demand of fleet group j during operating period t, d_{ow} is the one-way route distance, e_{EV} is the specific energy consumption of the electric shuttle van, and $n_{j,t}$ is the number of one-way trips assigned to fleet group j during the corresponding operating period. Using $d_{\mathrm{ow}} = 28$ km and $e_{\mathrm{EV}} = 0.187$ kWh/km, one one-way shuttle trip requires approximately 5.24 kWh of traction energy. During normal-semester operation, each van performs three one-way trips per day, equivalent to 84 km/day and 15.71 kWh/day per vehicle. Since each terminal-based fleet group consists of five vans, the normal daily charging demand is 78.54 kWh/day per station, or 157.08 kWh/day for the full 10-van fleet.

 doi:10.20944/preprints202605.0703.v1

During the reduced summer semester, only the HK-based group operates (10 trips/day; 52.36 kWh/day at HK), while the DS-based group is offline for maintenance. The combined annual demand is 15,341.5 kWh/yr at HK and 13,351.8 kWh/yr at DS, totaling 28,693.3 kWh/yr (≈28.69 MWh/yr).

Each van consumes only 17.5% of its 90 kWh battery per day, confirming that scheduled service can be completed without opportunity charging during the day.

Table 2. Technical specifications and energy consumption parameters of the selected electric shuttle van.

Specification	Value
Vehicle type	Electric shuttle van
Vehicle weight	2,239 kg
Battery capacity	90 kWh
Maximum driving range (NEDC)	570 km
Average energy consumption	18.7 kWh/100 km
Specific energy consumption, e_{EV}	0.187 kWh/km
Energy efficiency	5.3 km/kWh
One-way route distance	28 km
Energy per one-way trip	5.24 kWh/trip
Daily distance per van	84 km/day

2.3. Annual Energy Demand

Because the captive fleet has fixed routes and known operating days, the annual energy demand is computed deterministically rather than from stochastic arrival patterns:

The annual charging energy demand of fleet group j is expressed as

$$E_{\mathrm{ann},j} = d_{\mathrm{ow}} e_{\mathrm{EV}} \sum_{s \in \mathcal{S}} n_{j,s}\, T_s \qquad (2)$$

where $E_{\mathrm{ann},j}$ is the annual charging energy demand of fleet group j, d_{ow} is the one-way route distance, e_{EV} is the specific energy consumption of the electric shuttle van, $n_{j,s}$is the number of one-way trips per operating day for fleet group j in operating season s, and T_s is the number of operating days in that season. The set $\mathcal{S}$ includes the normal academic semester and the reduced summer-semester operation.

Each group performs 15 one-way trips/day in the normal semester, giving 78.54 kWh/day per station; in the summer semester, only HK operates with 10 trips/day (52.36 kWh/day) for 38 days while DS is offline.

The resulting annual demand is 15,341.5 kWh/yr at HK (53.5%) and 13,351.8 kWh/yr at DS (46.5%), totaling 28,693.3 kWh/yr (28.70 MWh/yr) (Table 3). The calendar-aware demand is ~50% lower than a naive 365-day extrapolation, providing a more realistic basis for PV–BESS sizing.

Table 3. Annual charging energy demand of the proposed electric shuttle fleet.

Station/Fleet Group	Normal semester demand	Summer semester demand	Operating calendar	E_{ann}	Share
Huay Kaew station—Van Group A	78.54 kWh/day	52.36 kWh/day	170 normal days + 38 summer days	15,341.5 kWh/yr	53.5%
Doi Saket station - Van Group B	78.54 kWh/day	0 kWh/day	170 normal days only	13,351.8 kWh/yr	46.5%
System total	157.08 kWh/day	52.36 kWh/day	208 operating days	28,693.3 kWh/yr	100%

 doi:10.20944/preprints202605.0703.v1

2.4. Siting Decision: One Centralized Station Versus Two Distributed Stations

Two charging-infrastructure layouts are compared for the 10-van fleet: (i) one centralized station at Huay Kaew (HK), and (ii) two distributed stations at HK and Doi Saket (DS). This subsection derives the dead-run distance and resulting non-revenue energy; the full economic comparison is in Section 3.1.

$$D_{\text{dead}} = 2d_{\text{ow}}N_{\text{DS}}T_{\text{N}} \tag{3}$$

and

$$E_{\text{dead}} = D_{\text{dead}}e_{\text{EV}} \tag{4}$$

where D_{dead} is the annual dead-run distance, d_{ow} is the one-way distance between the two campuses, N_{DS} is the number of Doi Saket-based vans, T_{N} is the number of normal-semester operating days, E_{dead} is the annual dead-run energy consumption, and e_{EV} is the specific energy consumption of the electric shuttle van.

For a single-station configuration, with $d_{\text{ow}} = 28$ km, $N_{\text{DS}} = 5$, $T_{\text{N}} = 170$ days, and $e_{\text{EV}} = 0.187$ kWh/km, the additional non-revenue travel would be 47,600 km/year, which corresponds to 8,901 kWh/year of unnecessary EV energy consumption. Thus, the annual energy demand for charging would increase from 28,693.3 kWh/year in the distributed case to 37,594.5 kWh/year in the centralized case, which is an increase of about 31.0%.

$$C_k = c_{\text{PV}}P_{\text{PV},k} + c_{\text{B}}E_{\text{BESS},k} + c_{\text{ch}}N_{\text{ch},k} + C_{\text{civ},k} \tag{5}$$

where C_k is the infrastructure cost of configuration k, c_{PV} is the PV installation cost, $P_{\text{PV},k}$ is the installed PV capacity, c_{B} is the BESS unit cost, $E_{\text{BESS},k}$ is the BESS capacity, c_{ch} is the charger unit cost, $N_{\text{ch},k}$ is the number of chargers, and $C_{\text{civ},k}$ represents civil and grid-connection costs. The adopted unit costs were USD 629/kWp for PV, USD 271/kWh for LFP BESS [24] 100 kWh LFP module, and USD 2,143 per 7.4 kW AC charger.

$$\Delta NPV = (C_{\text{cen}} - C_{\text{dist}}) + (B_{\text{dead}} + B_{\text{PV,DS}})\left[\frac{1-(1+r)^{-N}}{r}\right] + \frac{C_{\text{rep,cen}} - C_{\text{rep,dist}}}{(1+r)^{t_{\text{rep}}}} \tag{6}$$

where ΔNPV is the net present value advantage of the distributed two-station configuration relative to the centralized one-station configuration; C_{cen} and C_{dist} are the initial infrastructure costs of the centralized and distributed configurations, respectively; B_{dead} is the annual monetary benefit associated with avoided dead-run electricity consumption; $B_{\text{PV,DS}}$ is the annual monetary benefit of the additional 30 kWp PV system installed at the Doi Saket station; r is the discount rate; N is the project lifetime; $C_{\text{rep,cen}}$ and $C_{\text{rep,dist}}$ are the scheduled BESS replacement costs of the centralized and distributed configurations, respectively; and t_{rep} is the replacement year, which is taken as year 10 in this study.

In this formulation, the distributed-station advantage consists of two separable components: (i) the siting-only benefit from avoided dead-run travel and reduced centralized storage requirement, and (ii) the additional rooftop-PV opportunity at the DS station. To avoid overstating the siting effect alone, these components are reported separately in the results.

For a 15-year project lifetime and an 8% discount rate, the combined annual distributed-configuration benefit $(B_{\text{dead}} + B_{\text{PV,DS}})$ is approximately USD 3,909/year, giving a present value of approximately USD 33,457. The distributed configuration also provides an initial CAPEX saving of USD 3,286. In addition, the centralized configuration incurs a higher scheduled BESS replacement cost because it requires 300 kWh of storage, whereas the distributed configuration requires only 200 kWh. The corresponding year-10 replacement-cost difference is USD 27,143, with a discounted present value of approximately USD 12,571. Therefore, the total NPV advantage of the distributed configuration is approximately USD 49,313.

 doi:10.20944/preprints202605.0703.v1

The two-station distributed configuration is therefore selected as the baseline. Full economic comparison is in Section 3.1.

2.5. PV-BESS System Model

Following the distributed two-station configuration in Section 2.4, each station comprises a roof-mounted PV array, an LFP BESS, one 7.4 kW Level-2 AC charger, and a grid-backup connection. PV supplies daytime loads and charges the BESS, stored energy supports overnight EV charging, and the grid serves as backup. Figure 2 shows the architecture; both stations adopt the same structure because they share peak normal-semester demand of 78.54 kWh/day.

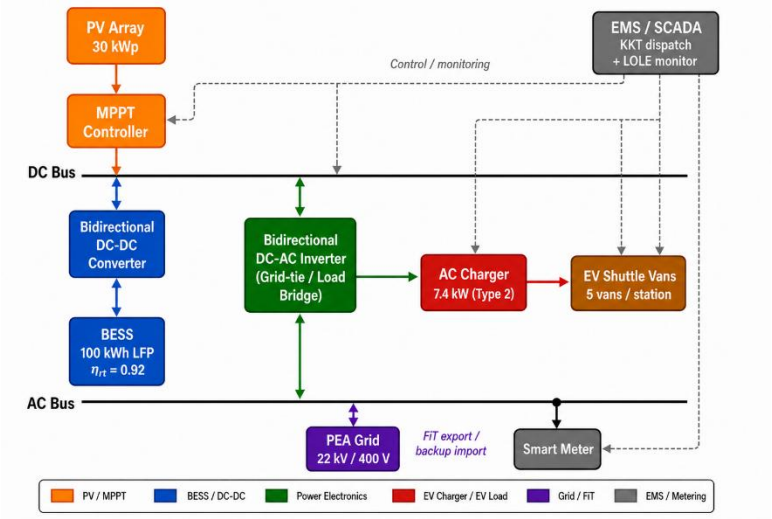

Figure 2. Block diagram of the hybrid PV–BESS electric vehicle charging station.

The daily PV energy output at station i is estimated using

$$E_{\mathrm{PV},i}^{\mathrm{day}} = P_{\mathrm{PV},i} H_{\mathrm{PSH}} PR \tag{7}$$

with H_{PSH}= 5.02 h/day and PR = 0.80, giving 120.48 kWh/day per 30 kWp station, or 43,975.2 kWh/yr (87,950.4 kWh/yr system).

Daily energy sufficiency compares the effective PV energy with station-level demand:

$$\eta_{\mathrm{BESS}} E_{\mathrm{PV},i}^{\mathrm{day}} \geq f_{\mathrm{sol}} E_{\mathrm{EV},i}^{\mathrm{day}} \tag{8}$$

Daily PV exceeds station demand of 78.54 kWh/day, providing margin for BESS charging and surplus.

BESS capacity follows the one-day autonomy requirement [28], accounting for round-trip efficiency and depth of discharge:

$$E_{\mathrm{BESS},i}^{\min} = \frac{E_{\mathrm{EV},i}^{\mathrm{day}}}{\eta_{\mathrm{BESS}} DOD} \tag{9}$$

with η_{BESS} = 0.92 and DoD = 0.90, the minimum is 94.85 kWh, rounded to a 100 kWh LFP module. Effective deliverable energy = 82.80 kWh, exceeding 78.54 kWh/day with ≈4.26 kWh reserve.

Charger adequacy ensures daily demand is supplied within the overnight window:

 doi:10.20944/preprints202605.0703.v1

$$P_{\mathrm{ch},i}^{\min} = \frac{E_{\mathrm{EV},i}^{\mathrm{day}}}{T_{\mathrm{ch}}} \tag{10}$$

For 78.54 kWh/day station demand, the required power is below the 7.4 kW Level-2 rating; one charger per station is sufficient.

Operationally, the five vans at each station charge sequentially from a single 7.4 kW connector; individual van charging time is approximately 78.54 / (5 × 7.4) = 2.12 h per van, and total sequential charging duration is 78.54 / 7.4 ≈ 10.61 h, fitting within the 12.33 h assumed overnight window with 1.72 h scheduling slack. A single connector-rotation event (manual or controller-driven) is required between vans. If a more aggressive turnaround or redundancy is desired, two 7.4 kW connectors per station would reduce sequential charging duration to ≈5.3 h at incremental CAPEX of USD 2,143/station; this option is evaluated in the discussion as a future upgrade path.

Annual PV generation exceeds annual EV charging demand, resulting in a system-level surplus of approximately 59,257.1 kWh/year. In the base-case financial model, this surplus is assigned an internal electricity-credit value of 2.20 THB/kWh, representing either campus self-consumption by nearby daytime loads or an institutional accounting credit. Because this value is policy- and site-dependent, zero-credit and reduced-credit cases are examined as sensitivity cases rather than assuming the credit as a guaranteed feed-in tariff.

The model defines two design variables per station: PV capacity and BESS energy. The baseline configuration is 30 kWp PV, 100 kWh LFP BESS, one 7.4 kW charger per station (60 kWp PV, 200 kWh BESS, two chargers system-level).

2.6. Optimization Problem Formulation

The PV–BESS sizing problem is a constrained NPV-maximization for two distributed stations, each with two continuous variables (PV in kWp; BESS in kWh). The objective and the seven governing constraints are detailed below; non-binding constraints are confirmed in the KKT analysis (Section 2.9).

For station i, where $i \in \{\mathrm{HK}, \mathrm{DS}\}$, the decision vector is defined as

$$\mathbf{x}_i = \begin{bmatrix} P_{\mathrm{PV},i} \\ E_{\mathrm{BESS},i} \end{bmatrix} \tag{11}$$

where $P_{\mathrm{PV},i}$ is the PV capacity and $E_{\mathrm{BESS},i}$ is the BESS energy capacity at station i. The objective is to maximize NPV over the project lifetime:

$$\max_{\mathbf{x}_i} \ \mathrm{NPV}_i = -C_{0,i} + \sum_{t=1}^{N} \frac{CF_{i,t}}{(1+r)^t} \tag{12}$$

where $C_{0,i}$ is initial investment, $CF_{i,t}$ is annual net cash flow in year y, r is discount rate, and N is project lifetime.

The annual net cash flow combines six terms: EV-charging substitution benefit, PV export/credit value, dead-run avoidance, O&M, residual grid cost, and the year-10 BESS replacement [26,27]:

$$CF_{i,t} = B_{\mathrm{EV},i,t} + B_{\mathrm{PV},i,t} + B_{\mathrm{dead},i,t} - C_{\mathrm{O\&M},i,t} - C_{\mathrm{grid},i,t} - \delta_t C_{\mathrm{rep},i,t} \tag{13}$$

where $B_{\mathrm{EV},i,t}$ is EV charging substitution, $B_{\mathrm{PV},i,t}$ is PV export/credit value, $B_{\mathrm{dead},i,t}$ is dead-run avoidance, $C_{\mathrm{O\&M},i,t}$ is O&M, $C_{\mathrm{grid},i,t}$ is residual grid cost, and $C_{\mathrm{rep},i,t}$ is the year-10 BESS replacement (binary 1 in year 10).

The initial investment combines PV, BESS, charger, and civil components:

 doi:10.20944/preprints202605.0703.v1

$$C_{0,i} = c_{\mathrm{PV}} P_{\mathrm{PV},i} + c_{\mathrm{B}} E_{\mathrm{BESS},i} + c_{\mathrm{ch}} N_{\mathrm{ch},i} + C_{\mathrm{civ},i} \tag{14}$$

with PV at USD 629/kWp, LFP BESS at USD 271/kWh, charger at USD 2,143/unit, and civil/grid at USD 7,143/station, giving USD 55,286 per station and USD 110,571 system-wide [28,29].

A year-10 BESS replacement follows the LFP warranty:

$$C_{\mathrm{rep,sys}} = \sum_{i \in \{\mathrm{HK,DS}\}} c_{\mathrm{B}}\, E_{\mathrm{BESS},i}^{\mathrm{prac}} \tag{15}$$

with 200 kWh × USD 271/kWh = USD 54,286, present value ≈USD 25,145 at r = 8%.

Seven constraints govern the optimization. C1 (LOLE reliability):

$$g_1(\mathbf{x}_i) = \mathrm{LOLE}_i - \mathrm{LOLE}_{\max} \le 0 \tag{16}$$

with $\mathrm{LOLE}_{\max}$ = 8 h/year.

$$g_2(\mathbf{x}_i) = COE_i - COE_{\mathrm{diesel}} \le 0 \tag{17}$$

with diesel-equivalent benchmark COE_{diesel} computed from diesel price, fuel economy, and EV consumption:

$$COE_{\mathrm{diesel}} = \frac{p_{\mathrm{diesel}}}{\eta_{\mathrm{diesel}} e_{\mathrm{EV}}} \tag{18}$$

with p_{diesel} = USD 1.383/L (48.4 THB/L at 35 THB/USD), η_{diesel} = 7.50 km/L, and e_{EV} = 0.187 kWh/km.

$$g_3(\mathbf{x}_i) = f_{\mathrm{sol}}^{\min} - f_{\mathrm{sol},i} \le 0 \tag{19}$$

where $f_{\mathrm{sol}}^{\min}$denotes the minimum required solar fraction. The achieved solar fraction is defined as:

$$f_{\mathrm{sol},i} = \frac{E_{\mathrm{PV}\to\mathrm{EV},i}}{E_{\mathrm{EV},i}^{\mathrm{ann}}} \tag{20}$$

where $E_{\mathrm{PV}\to\mathrm{EV},i}$ is the annual PV energy used for EV charging and $E_{\mathrm{EV},i}^{\mathrm{ann}}$ is the annual EV charging demand at station i.

$$g_4(\mathbf{x}_i) = \frac{E_{\mathrm{EV},i}^{\mathrm{day}}}{\eta_{\mathrm{BESS}} DOD} - E_{\mathrm{BESS},i} \le 0 \tag{21}$$

with $E_{\mathrm{EV},i}^{\mathrm{day}}$ = 78.54 kWh/day, η_{BESS} = 0.92, DOD = 0.90, giving the theoretical minimum 94.85 kWh/station, rounded up to 100 kWh.

$$g_5(\mathbf{x}_i) = \frac{E_{\mathrm{EV},i}^{\mathrm{day}}}{T_{\mathrm{ch}}} - P_{\mathrm{ch},i} \le 0 \tag{22}$$

with T_{ch} the overnight charging window and $P_{\mathrm{ch},i}$ the charger power. One 7.4 kW charger per station satisfies this constraint.

$$g_6(\mathbf{x}_i) = C_{0,i} - C_{\max} \le 0 \tag{23}$$

with budget ceiling USD 71,429; practical CAPEX USD 55,286 satisfies this with positive slack.

 doi:10.20944/preprints202605.0703.v1

$$g_7(\mathbf{x}_i) = P_{\mathrm{PV},i} - P_{\mathrm{PV}}^{\max} \le 0 \tag{24}$$

with $P_{\mathrm{PV}}^{\max}$ = 30 kWp/station based on available rooftop area.

The 30 kWp upper bound corresponds to approximately 200 m² of usable south-facing rooftop area at each terminal building (Huay Kaew shelter and Doi Saket parking shelter), assuming a panel-to-area ratio of 6.7 m²/kWp typical of monocrystalline silicon modules at 200 W/m² nameplate density. This estimate was derived from architectural drawings of the existing terminal shelters and confirmed by a site walk-around. Carport-style PV expansion above the parking apron could increase this ceiling but is excluded from the base-case analysis to keep CAPEX bounded.

$$\begin{aligned} \max_{\mathbf{x}_i} \quad & \mathrm{NPV}_i(P_{\mathrm{PV},i}, E_{\mathrm{BESS},i}) \\ \text{s. t.} \quad & g_m(\mathbf{x}_i) \le 0, m = 1, \ldots, 7, \\ & P_{\mathrm{PV},i} \ge 0, \\ & E_{\mathrm{BESS},i} \ge 0. \end{aligned} \tag{25}$$

$$\max_{\mathbf{x}_{\mathrm{sys}}} \mathrm{NPV}_{\mathrm{sys}} = \sum_{i \in \{\mathrm{HK,DS}\}} \mathrm{NPV}_i \tag{26}$$

$$\mathbf{x}_{\mathrm{sys}} = \left[P_{\mathrm{PV,HK}}, E_{\mathrm{BESS,HK}}, P_{\mathrm{PV,DS}}, E_{\mathrm{BESS,DS}}\right]^T. \tag{27}$$

Both stations share peak demand and rooftop limit; the station-level KKT solution is symmetric and the system configuration doubles the station result:

$$P_{\mathrm{PV,HK}}^* = P_{\mathrm{PV,DS}}^*, E_{\mathrm{BESS,HK}}^* = E_{\mathrm{BESS,DS}}^*. \tag{28}$$

The resulting practical configuration is 60 kWp PV, 200 kWh LFP BESS, and two 7.4 kW AC chargers.

2.7. LOLE Probabilistic Model

Reliability is evaluated using loss of load expectation (LOLE), defined as the expected annual duration during which a station cannot fully supply scheduled EV charging from PV, BESS, and grid backup. Both stations share the same configuration and demand, so the assessment is performed at the station level.

Daily solar-resource uncertainty is represented by a log-normal PSH distribution:

$$H_d \sim \mathrm{LogNormal}(\mu_H, \sigma_H^2) \tag{29}$$

with mean $\bar{H} = 5.02$ h/day and CV_H = 0.10, giving log-normal parameters μ_H and σ_H^2.

$$\sigma_H^2 = \ln\left(1 + CV_H^2\right), \mu_H = \ln\left(\bar{H}\right) - \frac{1}{2}\sigma_H^2. \tag{30}$$

For each simulated day, the PV energy generated at station i is calculated as

$$E_{\mathrm{PV},i,d} = P_{\mathrm{PV},i} H_d PR \tag{31}$$

with installed PV capacity $P_{\mathrm{PV},i}$ and performance ratio PR; effective PV after BESS round-trip:

$$E_{\mathrm{PV,eff},i,d} = \eta_{\mathrm{BESS}} E_{\mathrm{PV},i,d} \tag{32}$$

with η_{BESS} = 0.92.

 doi:10.20944/preprints202605.0703.v1

Usable BESS energy follows the nominal capacity and depth of discharge:

$$E_{\mathrm{BESS},i}^{\mathrm{use}} = E_{\mathrm{BESS},i} DOD. \tag{33}$$

For the 100 kWh LFP BESS at $DOD = 0.90$, the usable capacity is 90.0 kWh. After accounting for BESS round-trip efficiency ($\eta_{\mathrm{BESS}} = 0.92$), the effective deliverable energy is 82.80 kWh, which exceeds the maximum daily station demand of 78.54 kWh/day. Grid availability is represented by a probability $p_g = 0.995$, reflecting the high availability of institutional distribution feeders in Chiang Mai. Because the BESS one-day autonomy provides the primary reliability buffer and the grid acts only as backup, the grid-availability assumption has limited influence on the deterministic sizing result.

Grid availability is modelled as a Bernoulli random variable:

$$A_{g,d} \sim \mathrm{Bernoulli}(p_g) \tag{34}$$

where $A_{g,d} = 1$ indicates that the grid is available on day d, $A_{g,d} = 0$ indicates a grid outage, and p_g is the grid-availability probability. The available grid energy in the charging window is

$$E_{\mathrm{grid},i,d}^{\mathrm{avail}} = A_{g,d} P_{\mathrm{ch},i} T_{\mathrm{ch}} \tag{35}$$

with one 7.4 kW charger and 12.33 h overnight window, max grid backup = 91.24 kWh/night > 78.54 kWh/day demand.

BESS state is simulated recursively over the synthetic horizon; daily unserved charging energy and equivalent loss-of-load duration are computed; annual LOLE is averaged over a 30-year synthetic simulation:

$$S_{i,d}^{+} = \min\left[E_{\mathrm{BESS},i}^{\mathrm{use}}, S_{i,d}^{-} + E_{\mathrm{PV,eff},i,d}\right] \tag{36}$$

BESS energy is updated each day; daily unserved charging energy is then computed:

$$E_{\mathrm{unserved},i,d} = \max\left[0, E_{\mathrm{EV},i}^{\mathrm{day}} - S_{i,d}^{+} - E_{\mathrm{grid},i,d}^{\mathrm{avail}}\right] \tag{37}$$

with $E_{\mathrm{EV},i}^{\mathrm{day}}$ the daily demand. Daily loss-of-load duration:

$$h_{\mathrm{loss},i,d} = \frac{E_{\mathrm{unserved},i,d}}{P_{\mathrm{ch},i}}. \tag{38}$$

Annual LOLE is averaged over the simulation horizon:

$$\mathrm{LOLE}_i = \frac{365}{D} \sum_{d=1}^{D} h_{\mathrm{loss},i,d} \tag{39}$$

with D = 30 years; constraint:

$$\mathrm{LOLE}_i \leq \mathrm{LOLE}_{\max} \tag{40}$$

with $\mathrm{LOLE}_{\max}$ = 8 h/year.

For the distributed design (30 kWp PV, 100 kWh LFP BESS, one 7.4 kW charger per station), the effective deliverable BESS energy (82.80 kWh) and grid-backup capacity (91.24 kWh/night) both exceed the maximum daily station demand (78.54 kWh). A loss-of-load event therefore requires a compound adverse condition; the resulting LOLE is well below the 8 h/year threshold and the reliability constraint is non-binding.

 doi:10.20944/preprints202605.0703.v1

2.8. Rationale for Selecting the KKT Approach

The optimization method was selected according to the mathematical structure of the revised PV–BESS sizing problem. After the siting analysis, the charging infrastructure is represented by two distributed stations located at the Huay Kaew and Doi Saket terminals. Each station serves the same peak normal-semester daily charging demand and is described by two continuous design variables: PV capacity, $P_{\mathrm{PV},i}$, and BESS capacity, $E_{\mathrm{BESS},i}$. This low-dimensional structure makes the problem suitable for analytical optimization rather than relying solely on numerical search.

For each station, the feasible design domain can be expressed as

$$\mathcal{X}_i = \left\{ (P_{\mathrm{PV},i}, E_{\mathrm{BESS},i}) \;\middle|\; g_m(\mathbf{x}_i) \le 0,\ m = 1, \ldots, 7 \right\} \tag{41}$$

where $g_m(\mathbf{x}_i)$ represents the seven technical, operational, and economic constraints defined in Section 2.6. Among these constraints, two have direct physical control over the optimal sizing boundary. The BESS autonomy constraint defines the minimum storage capacity required to satisfy one complete day of station-level charging demand:

$$E_{\mathrm{BESS},i} \ge \frac{E_{\mathrm{EV},i}^{\mathrm{day}}}{\eta_{\mathrm{BESS}} DOD} \tag{42}$$

and the PV rooftop-area constraint:

$$P_{\mathrm{PV},i} \le P_{\mathrm{PV}}^{\max}. \tag{43}$$

The Karush–Kuhn–Tucker (KKT) approach is selected as an analytical active-constraint tool for three reasons: (i) the problem is low-dimensional with two station-level variables; (ii) the objective function has a verified monotonic boundary structure over the feasible region; and (iii) the governing constraints are algebraic and physically interpretable. In this formulation, global optimality is not claimed from the KKT conditions alone; rather, it follows from the monotonic boundary argument, while the KKT multipliers identify which constraints are active at the resulting boundary solution. The Lagrangian for the station-level maximization problem is:

$$\mathcal{L}(\mathbf{x}_i, \boldsymbol{\lambda}) = \mathrm{NPV}_i(\mathbf{x}_i) - \sum_{m=1}^{7} \lambda_m \, g_m(\mathbf{x}_i), \tag{44}$$

where λ_m is the Lagrange multiplier associated with constraint g_m. At the optimum, the solution must satisfy stationarity, primal feasibility, dual feasibility, and complementary slackness:

$$\nabla_{\mathbf{x}_i} \mathcal{L}(\mathbf{x}_i^*, \boldsymbol{\lambda}^*) = 0, \tag{45}$$

$$g_m(\mathbf{x}_i^*) \le 0, \lambda_m^* \ge 0, \tag{46}$$

$$\lambda_m^* g_m(\mathbf{x}_i^*) = 0, m = 1, \ldots, 7. \tag{47}$$

A positive multiplier indicates that the corresponding constraint is binding; a zero multiplier indicates inactivity. For the present problem, the BESS autonomy and PV rooftop-area constraints are anticipated to be active, giving:

$$E_{\mathrm{BESS},i}^* = \frac{E_{\mathrm{EV},i}^{\mathrm{day}}}{\eta_{\mathrm{BESS}} DOD}, \tag{48}$$

$$P_{\mathrm{PV},i}^* = P_{\mathrm{PV}}^{\max}. \tag{49}$$

 doi:10.20944/preprints202605.0703.v1

The methodological workflow is summarized in Figure 3, comprising route and fleet characterization, energy-demand modelling, siting analysis, PV–BESS system modelling, constrained optimization, KKT solution, Differential Evolution verification, and Monte Carlo financial robustness analysis.

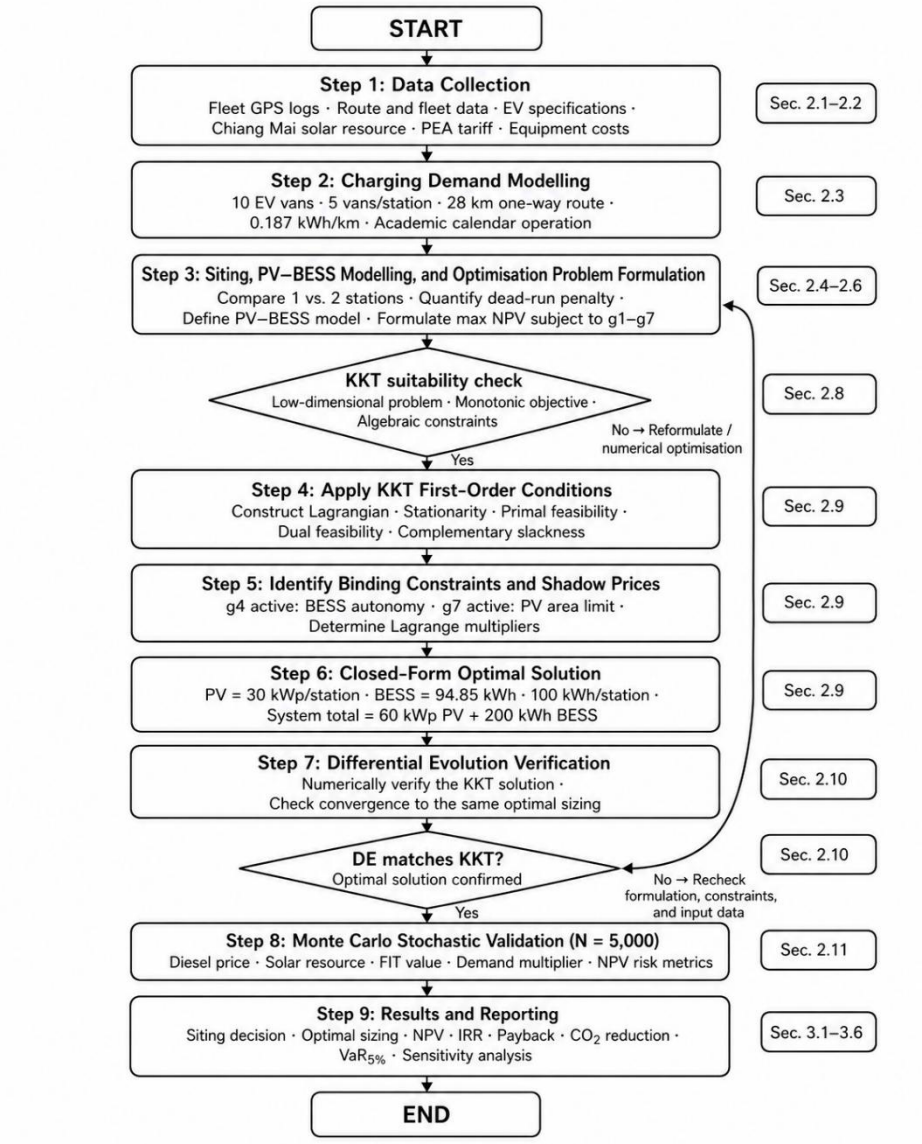

Figure 3. Methodology flowchart for KKT-based optimal PV–BESS sizing of the RMUTL electric academic shuttle charging stations.

Table 4 compares KKT with alternative optimization methods (e.g., MILP, metaheuristics, HOMER-based simulation [29]) for this problem class.

Table 4. Comparison of optimization approaches for the PV–BESS sizing problem.

Method	Active-constraint certificate	Binding Constraints Identified	Shadow Prices Available	Closed-Form Result
KKT (this work)	Suitable for the revised low-dimensional problem after monotonicity and	g_4: BESS autonomy and g_7: PV area limit identified as active	λ_4 and λ_7 provide marginal values of the active constraints	$P^*_{\mathrm{PV},i} = P^{\max}_{\mathrm{PV}}$, $E^*_{\mathrm{BESS},i} = E^{\mathrm{day}}_{\mathrm{EV},i}/(\eta_{\mathrm{BESS}} DOD)$

 doi:10.20944/preprints202605.0703.v1

	active-constraint verification			
Differential Evolution / PSO / GA	Useful for numerical verification or global search	Not directly	No	No
Interior-Point / SQP	Provides numerical constrained optimum	Possible numerically, but not explicit	Limited for engineering interpretation	No
Linear Programming (LP)	Provides exact optimum if the problem is fully linearized	Yes, after linearization	Yes	No, unless the full problem is reformulated as linear
HOMER / simulation-based sizing	Useful for techno-economic screening	Not explicit	No	No

2.9. KKT Analytical Solution

The KKT analytical solution was derived at the station level for the distributed charging configuration. Because the Huay Kaew and Doi Saket stations serve the same peak normal-semester daily charging demand and have the same rooftop PV installation limit, the two stations have identical optimization structures. It is therefore sufficient to derive the closed-form solution for a representative station i, where $i \in \{\mathrm{HK}, \mathrm{DS}\}$. The resulting solution is then applied symmetrically to both stations.

The station-level optimization problem is to maximize the net present value,

$$\max_{\mathbf{x}_i} \ \mathrm{NPV}_i\left(P_{\mathrm{PV},i}, E_{\mathrm{BESS},i}\right), \tag{50}$$

subject to the seven constraints from Section 2.6. The KKT analysis focuses on the two constraints that bound the sizing region—BESS one-day autonomy and PV rooftop-area:

$$g_4(\mathbf{x}_i) = \frac{E_{\mathrm{EV},i}^{\mathrm{day}}}{\eta_{\mathrm{BESS}} DOD} - E_{\mathrm{BESS},i} \le 0, \tag{51}$$

$$g_7(\mathbf{x}_i) = P_{\mathrm{PV},i} - P_{\mathrm{PV}}^{\max} \le 0. \tag{52}$$

Here, $E_{\mathrm{EV},i}^{\mathrm{day}}$ is the maximum daily charging demand at station i, η_{BESS} is the BESS round-trip efficiency, DOD is the allowable depth of discharge, and $P_{\mathrm{PV}}^{\max}$ is the maximum PV capacity permitted by the available rooftop area.

Proposition 1. For the deterministic station-level sizing problem, if $\partial NPV_i / \partial P_{\mathrm{PV},i} > 0$ for $0 \le P_{\mathrm{PV},i} \le P_{\mathrm{PV}}^{\max}$, and $\partial NPV_i / \partial E_{\mathrm{BESS},i} < 0$ for $E_{\mathrm{BESS},i} \ge E_{\mathrm{EV},i}^{\mathrm{day}} / (\eta_{\mathrm{BESS}} DOD)$, then the NPV-maximizing feasible solution is located at the intersection of the PV upper bound and the BESS minimum-autonomy boundary. Under these conditions, the station-level optimum is $P_{\mathrm{PV},i}^{*} = P_{\mathrm{PV}}^{\max}, E_{\mathrm{BESS},i}^{*} = \frac{E_{\mathrm{EV},i}^{\mathrm{day}}}{\eta_{\mathrm{BESS}} DOD}$. The KKT conditions provide an active-constraint certificate for this boundary solution, while Differential Evolution is used as an independent numerical verification.

The Lagrangian for these two governing constraints is:

 doi:10.20944/preprints202605.0703.v1

$$\mathcal{L} = \mathrm{NPV}_i - \lambda_4 \left(\frac{E_{\mathrm{EV},i}^{\mathrm{day}}}{\eta_{\mathrm{BESS}} DOD} - E_{\mathrm{BESS},i} \right) - \lambda_7 \left(P_{\mathrm{PV},i} - P_{\mathrm{PV}}^{\max} \right), \tag{53}$$

where λ_4 and λ_7 are the Lagrange multipliers associated with the BESS autonomy and PV rooftop-area constraints, respectively.

The stationarity conditions are

$$\frac{\partial \mathcal{L}}{\partial P_{\mathrm{PV},i}} = \frac{\partial \mathrm{NPV}_i}{\partial P_{\mathrm{PV},i}} - \lambda_7 = 0, \tag{54}$$

$$\frac{\partial \mathcal{L}}{\partial E_{\mathrm{BESS},i}} = \frac{\partial \mathrm{NPV}_i}{\partial E_{\mathrm{BESS},i}} + \lambda_4 = 0. \tag{55}$$

The marginal NPV of PV capacity is positive within the feasible range because additional PV generation offsets EV charging energy, supports campus self-consumption, or earns electricity-credit value:

$$\frac{\partial \mathrm{NPV}_i}{\partial P_{\mathrm{PV},i}} = 365 H_{\mathrm{PSH}} PR v_{\mathrm{PV}} A_N - c_{\mathrm{PV}}, \tag{56}$$

where H_{PSH} is the average peak sun hour, PR is the PV performance ratio, v_{PV} is the electricity value assigned to PV generation, A_N is the present-value annuity factor over the project lifetime, and c_{PV} is the PV installation cost. Under the adopted base-case assumptions, this derivative remains positive. Therefore, from Eq. (54), $\lambda_7 > 0$, indicating that the PV rooftop-area constraint is active. The optimal PV capacity is consequently obtained at the upper bound:

$$P_{\mathrm{PV},i}^{*} = P_{\mathrm{PV}}^{\max}. \tag{57}$$

With $P_{\mathrm{PV}}^{\max} = 30$ kWp per terminal, the optimal PV capacity is

$$P_{\mathrm{PV},i}^{*} = 30 \text{ kWp/station}. \tag{58}$$

Conversely, the marginal NPV of BESS capacity becomes negative once the autonomy requirement is satisfied: additional storage adds CAPEX, replacement cost, and O&M but does not increase the scheduled EV demand. By Eq. (55), this implies a positive multiplier and the autonomy constraint is active:

$$\frac{\partial \mathrm{NPV}_i}{\partial E_{\mathrm{BESS},i}} < 0 \text{for} E_{\mathrm{BESS},i} > \frac{E_{\mathrm{EV},i}^{\mathrm{day}}}{\eta_{\mathrm{BESS}} DOD}. \tag{59}$$

From Eq. (55), this implies $\lambda_4 > 0$, so the BESS autonomy constraint is active. The optimal BESS capacity is therefore obtained at the minimum feasible autonomy boundary:

$$E_{\mathrm{BESS},i}^{*} = \frac{E_{\mathrm{EV},i}^{\mathrm{day}}}{\eta_{\mathrm{BESS}} DOD}. \tag{60}$$

Using $E_{\mathrm{EV},i}^{\mathrm{day}} = 78.54$ kWh/day, $\eta_{\mathrm{BESS}} = 0.92$, and $DOD = 0.90$, the theoretical BESS requirement is

$$E_{\mathrm{BESS},i}^{*} = 94.85 \text{ kWh/station}. \tag{61}$$

The theoretical value is rounded up to the nearest commercially available LFP module:

 doi:10.20944/preprints202605.0703.v1

$$E_{\mathrm{BESS},i}^{\mathrm{prac}} = 100\ \mathrm{kWh/station}. \tag{62}$$

The corresponding effective deliverable BESS energy is

$$E_{\mathrm{BESS},i}^{\mathrm{eff}} = E_{\mathrm{BESS},i}^{\mathrm{prac}} DOD\eta_{\mathrm{BESS}} = 82.80\ \mathrm{kWh}. \tag{63}$$

This exceeds the maximum daily demand (78.54 kWh/day), giving an operational reserve of ≈4.26 kWh (5.4%).

The complementary slackness conditions for the two active constraints are

$$\lambda_4 \left(\frac{E_{\mathrm{EV},i}^{\mathrm{day}}}{\eta_{\mathrm{BESS}} DOD} - E_{\mathrm{BESS},i}^{*} \right) = 0, \tag{64}$$

$$\lambda_7 \left(P_{\mathrm{PV},i}^{*} - P_{\mathrm{PV}}^{\max} \right) = 0. \tag{65}$$

Since $\lambda_4 > 0$ and $\lambda_7 > 0$, both constraints are binding at the optimum. The remaining five constraints—LOLE reliability, cost-of-energy competitiveness, minimum solar fraction, charger adequacy, and station-level budget—are satisfied with positive slack and therefore have zero multipliers:

$$\lambda_m = 0, m \in \{1,2,3,5,6\}. \tag{66}$$

The monotonic boundary analysis, together with the KKT complementary-slackness conditions, identifies the station-level solution at the intersection of the BESS minimum-autonomy boundary and the PV maximum-area boundary:

$$\left(P_{\mathrm{PV},i}^{*}, E_{\mathrm{BESS},i}^{*} \right) = (30\ \mathrm{kWp}, 94.85\ \mathrm{kWh}). \tag{67}$$

This result should be interpreted as a global optimum within the deterministic station-level model under the stated monotonicity and feasibility assumptions, rather than as a consequence of the KKT conditions alone. The KKT multipliers indicate that g_4 and g_7 are active, while the remaining constraints are satisfied with positive slack. The engineering implication is that PV capacity should be maximized up to the rooftop limit, whereas BESS capacity should be limited to the minimum one-day autonomy requirement.

After commercial rounding of the BESS capacity, the practical station-level design becomes

$$\left(P_{\mathrm{PV},i}^{\mathrm{prac}}, E_{\mathrm{BESS},i}^{\mathrm{prac}} \right) = (30\ \mathrm{kWp}, 100\ \mathrm{kWh}). \tag{68}$$

Both stations being symmetric, the system-level configuration is twice the station-level result:

$$P_{\mathrm{PV,sys}}^{\mathrm{prac}} = 60\ \mathrm{kWp}, \qquad E_{\mathrm{BESS,sys}}^{\mathrm{prac}} = 200\ \mathrm{kWh}. \tag{69}$$

The analytical solution has direct engineering meaning: maximize PV up to the rooftop limit because additional generation has positive marginal value and minimize BESS to the one-day autonomy boundary because additional storage adds lifecycle cost without increasing scheduled demand.

 doi:10.20944/preprints202605.0703.v1

2.10. Differential Evolution Verification

Differential Evolution (DE) [21] was used as independent numerical verification of the closed-form KKT solution. The purpose was to confirm that a stochastic global search recovers the same optimum without prior knowledge of the active constraints.

For each distributed charging station i, the DE decision vector was defined as

$$\mathbf{x}_i^{\mathrm{DE}} = \begin{bmatrix} P_{\mathrm{PV},i} \\ E_{\mathrm{BESS},i} \end{bmatrix}, \tag{70}$$

where $P_{\mathrm{PV},i}$ is the installed PV capacity and $E_{\mathrm{BESS},i}$ is the BESS energy capacity. The DE algorithm was formulated as a minimization problem by minimizing the negative station-level NPV with an exterior penalty for constraint violation:

$$\min_{\mathbf{x}_i^{\mathrm{DE}}} \Phi_i(\mathbf{x}_i^{\mathrm{DE}}) = -\mathrm{NPV}_i(\mathbf{x}_i^{\mathrm{DE}}) + \rho \sum_{m=1}^{7} [\max\left(0, g_m\left(\mathbf{x}_i^{\mathrm{DE}}\right)\right)]^2 \tag{71}$$

where Φ_i is the penalised objective function, $g_m\left(\mathbf{x}_i^{\mathrm{DE}}\right)$ represents the seven constraints defined in Section 2.6, and ρ is a large penalty coefficient used to reject infeasible candidate solutions. This formulation allows the DE search to explore the full feasible design space while strongly penalising candidates that violate reliability, cost, solar-fraction, autonomy, charger, budget, or rooftop-area constraints.

Search bounds covered the physically meaningful design range; the upper PV bound matched the rooftop limit and the BESS upper bound was deliberately set well above the one-day autonomy requirement to test whether oversized storage could improve NPV.

$$0 \le P_{\mathrm{PV},i} \le 30\ \mathrm{kWp}, \tag{72}$$

$$0 \le E_{\mathrm{BESS},i} \le 200\ \mathrm{kWh}. \tag{73}$$

The DE algorithm was implemented using the DE/rand/1/bin strategy. The population size was set to 20 individuals, the mutation factor was randomly varied within the interval $F \in [0.5, 0.9]$, and the crossover probability was set to $CR = 0.9$. The maximum number of generations was 300. A fixed random seed was used to ensure reproducibility, and convergence was declared when the change in the best penalised objective value became negligible over consecutive generations.

DE converged to the same station-level solution as the KKT analytical derivation, with the BESS value matching the closed-form autonomy expression. The continuous BESS optimum is rounded up to a 100 kWh module, giving a verified station-level configuration of 30 kWp PV and 100 kWh LFP BESS, and a system-level configuration of 60 kWp PV and 200 kWh BESS for the two distributed stations.

$$P_{\mathrm{PV},i}^{\mathrm{DE}} = 30.00\ \mathrm{kWp}, \tag{74}$$

$$E_{\mathrm{BESS},i}^{\mathrm{DE}} = 94.85\ \mathrm{kWh}. \tag{75}$$

$$E_{\mathrm{BESS},i}^{\mathrm{DE}} = \frac{E_{\mathrm{EV},i}^{\mathrm{day}}}{\eta_{\mathrm{BESS}} DOD}. \tag{76}$$

$$E_{\mathrm{BESS},i}^{\mathrm{prac}} = 100\ \mathrm{kWh}. \tag{77}$$

 doi:10.20944/preprints202605.0703.v1

$$P_{\mathrm{PV},i}^{\mathrm{prac}} = 30\ \mathrm{kWp}, \qquad E_{\mathrm{BESS},i}^{\mathrm{prac}} = 100\ \mathrm{kWh}. \tag{78}$$

$$P_{\mathrm{PV,sys}}^{\mathrm{prac}} = 60\ \mathrm{kWp}, \quad E_{\mathrm{BESS,sys}}^{\mathrm{prac}} = 200\ \mathrm{kWh}. \tag{79}$$

Agreement between DE and the closed-form boundary solution confirms numerical consistency and supports the identified active-constraint structure. Because DE is a stochastic global-search method rather than a formal proof of optimality, this result is used as numerical verification that no better feasible solution was found within the prescribed search bounds.

2.11. Stochastic NPV Model

A stochastic NPV model evaluates financial robustness of the fixed optimal two-station design (30 kWp PV, 100 kWh LFP BESS per station). Capacities are not re-optimized in each scenario; only financial outcomes vary.

For each Monte Carlo scenario s, where $s = 1, \dots, N_s$, the stochastic input vector is defined as

$$\boldsymbol{\theta}_s = \left[p_{d,0}^{(s)}, g_d^{(s)}, H_{\mathrm{PSH}}^{(s)}, M_D^{(s)}, v_{\mathrm{PV}}^{(s)}, M_{\mathrm{O\&M}}^{(s)}, r^{(s)}\right], \tag{80}$$

where $p_{d,0}^{(s)}$ is the initial diesel price, $g_d^{(s)}$ is the annual diesel-price escalation rate, $H_{\mathrm{PSH}}^{(s)}$ is the daily peak sun hour, $M_D^{(s)}$ is the fleet-utilization multiplier, $v_{\mathrm{PV}}^{(s)}$ is the PV electricity-credit or internal campus energy value, $M_{\mathrm{O\&M}}^{(s)}$ is the operation-and-maintenance cost multiplier, and $r^{(s)}$ is the discount rate. These variables represent the dominant uncertainty sources affecting the lifecycle value of the project: fuel price, solar resource, fleet utilization, PV surplus valuation, maintenance cost, and cost of capital.

$$p_{d,0}^{(s)} \sim \mathcal{N}_{[0.6,\infty)}(1.383, 0.15^2), \tag{81}$$

$$g_d^{(s)} \sim \mathcal{N}(0.03, 0.015^2), \tag{82}$$

$$H_{\mathrm{PSH}}^{(s)} \sim \mathrm{LogNormal}(\mu_H, \sigma_H^2), \tag{83}$$

$$M_D^{(s)} \sim Triangular(0.85, 1.00, 1.15), \tag{84}$$

$$v_{\mathrm{PV}}^{(s)} \sim Triangular(1.70, 2.20, 2.70), \tag{85}$$

$$M_{\mathrm{O\&M}}^{(s)} \sim \mathcal{N}_{[0,\infty)}(1.00, 0.10^2), \tag{86}$$

$$r^{(s)} \sim \mathcal{N}_{[0.04,0.12]}(0.08, 0.01^2). \tag{87}$$

The log-normal solar-resource parameters μ_H and σ_H are defined from the mean peak sun hour of Chiang Mai and the assumed coefficient of variation, as described in the LOLE model. Normal

 doi:10.20944/preprints202605.0703.v1

distributions are truncated at physically meaningful bounds to avoid negative or implausible values. In particular, the discount rate is truncated to $0.04 \le r \le 0.12$, representing a plausible Thai institutional WACC range.

Annual EV demand (28,693.3 kWh/yr) is scaled by $M_D^{(s)}$, PV generation applies a 0.5%/yr degradation, and avoided diesel is computed from scenario shuttle distance, with annual diesel-price escalation:

$$E_{\mathrm{EV},i}^{\mathrm{ann},(s)} = M_D^{(s)} E_{\mathrm{EV},i}^{\mathrm{ann}}. \tag{88}$$

Annual PV generation at station i in year $t$is calculated as

$$E_{\mathrm{PV},i,t}^{(s)} = 365 P_{\mathrm{PV},i} H_{\mathrm{PSH}}^{(s)} PR (1-\delta_{\mathrm{PV}})^{t-1}, \tag{89}$$

where $P_{\mathrm{PV},i} = 30$ kWp, PR is the PV performance ratio, and δ_{PV} is the annual PV degradation rate. The annual PV surplus available for campus self-consumption or export credit is then estimated as

$$E_{\mathrm{sur},i,t}^{(s)} = \max\left[0, E_{\mathrm{PV},i,t}^{(s)} - E_{\mathrm{EV},i}^{\mathrm{ann},(s)}\right]. \tag{90}$$

$$F_{d,t}^{(s)} = \frac{D_{\mathrm{ann}}^{(s)}}{\eta_{\mathrm{diesel}}}, \tag{91}$$

where $D_{\mathrm{ann}}^{(s)}$ is the annual shuttle distance adjusted by $M_D^{(s)}$, and η_{diesel} is the diesel fuel economy in km/L. The diesel price in year $t$is escalated according to

$$p_{d,t}^{(s)} = p_{d,0}^{(s)} (1+g_d^{(s)})^{t-1}. \tag{92}$$

The annual net cash flow of scenario $s$is calculated as

$$CF_t^{(s)} = F_{d,t}^{(s)} p_{d,t}^{(s)} + S_{\mathrm{O\&M},t}^{(s)} + v_{\mathrm{PV}}^{(s)} \sum_i E_{\mathrm{sur},i,t}^{(s)} - C_{\mathrm{grid},t}^{(s)} - C_{\mathrm{O\&M},t}^{(s)} - \delta_{t,t_{\mathrm{rep}}} C_{\mathrm{rep}}^{(s)}, \tag{93}$$

where $S_{\mathrm{O\&M},t}^{(s)}$ is the maintenance-cost saving from replacing diesel vans with electric vans, $C_{\mathrm{grid},t}^{(s)}$ is the residual grid-electricity cost, $C_{\mathrm{O\&M},t}^{(s)}$ is the annual operation and maintenance cost of the PV–BESS charging infrastructure, $C_{\mathrm{rep}}^{(s)}$ is the scheduled BESS replacement cost, and $\delta_{t,t_{\mathrm{rep}}}$ is a binary indicator equal to 1 in the replacement year and 0 otherwise. In the revised design, the scheduled BESS replacement is applied in year $t_{\mathrm{rep}} = 10$. Based on the installed system-level BESS capacity of 200 kWh and the adopted LFP BESS unit cost of 9,500 THB/kWh, the replacement cost is $C_{\mathrm{rep}} = 1.90$ million THB, equivalent to USD 54,286. This cost is treated as a year-10 cash outflow in each Monte Carlo scenario and discounted using the scenario-specific discount rate $r^{(s)}$.

The stochastic NPV for scenario $s$is then expressed as

$$\mathrm{NPV}^{(s)} = -C_0 + \sum_{t=1}^{N} \frac{CF_t^{(s)}}{\left(1+r^{(s)}\right)^t}, \tag{94}$$

 doi:10.20944/preprints202605.0703.v1

where C_0 is the total incremental initial investment, $N = 15$ years is the project lifetime, and $r^{(s)}$ is the scenario-specific discount rate.

The NPV distribution is evaluated using expected NPV, P(NPV > 0), 5th-percentile VaR, and CVaR (mean over the 5% worst scenarios) [30]:

$$\mathbb{E}[\mathrm{NPV}] = \frac{1}{N_s}\sum_{s=1}^{N_s} \mathrm{NPV}^{(s)}, \tag{95}$$

$$P(\mathrm{NPV} > 0) = \frac{1}{N_s}\sum_{s=1}^{N_s} \mathbf{1}\left[\mathrm{NPV}^{(s)} > 0\right], \tag{96}$$

where $\mathbf{1}[\cdot]$ is the indicator function. The 5th-percentile value-at-risk is defined as

$$VaR_{5\%} = Q_{0.05}\left(\mathrm{NPV}^{(s)}\right), \tag{97}$$

where $Q_{0.05}$ denotes the 5th percentile of the simulated NPV distribution. The conditional value-at-risk is calculated as

$$CVaR_{5\%} = \mathbb{E}\left[\mathrm{NPV}^{(s)} \mid \mathrm{NPV}^{(s)} \le VaR_{5\%}\right]. \tag{98}$$

A total of $N_s = 5{,}000$ Monte Carlo scenarios was used. Convergence was verified by monitoring the standard error of the mean NPV, and the sample size was considered sufficient when the 95% confidence interval of the mean stabilized. This stochastic formulation complements the deterministic KKT and DE results by quantifying the downside financial risk of the fixed optimal PV–BESS design under uncertainty in diesel price, fuel escalation, solar resource, fleet utilization, PV electricity value, operation and maintenance cost, and discount rate, as shown in Table 5. The resulting NPV distribution and risk metrics are reported in Section 3.5.

Table 5. Monte Carlo input distributions for the 5,000-scenario stochastic NPV analysis.

Parameter	Symbol	Distribution	Mean / mode	σ / range	Source / justification
Initial diesel price	$p_{d,0}$	Normal, truncated at $p_{d,0} \geq 0.6$USD/L	1.383 USD/L	$\sigma = 0.150$USD/L	Thai Oil retail diesel 2023–2025 envelope; ±20% tornado bound
Diesel escalation rate	g_d	Normal	3.0%/yr	$\sigma = 1.5$%/yr	Thai diesel CPI 2010–2024; consistent with IEA STEPS
Daily peak sun hour	H_{PSH}	Log-normal	5.02 h/day	$CV = 0.10$	NSRDB Chiang Mai 2010–2020 [6]
Fleet-utilization multiplier	M_D	Triangular	1.00	[0.85, 1.15]	±15% deviation from nominal academic-calendar service
PV electricity-credit value	v_{PV}	Triangular	2.20 THB/kWh	[1.70, 2.70]	Internal campus electricity-credit ±0.50 THB/kWh

 doi:10.20944/preprints202605.0703.v1

O&M cost multiplier	$M_{\mathrm{O\&M}}$	Normal, truncated at $M_{\mathrm{O\&M}} \geq 0$	1.00	$\sigma = 0.10$	Manufacturer warranty + PNNL 2020 [26]
Discount rate	r	Normal, truncated to $0.04 \leq r \leq 0.12$	8.0%	$\sigma = 1.0\%$	Thai institutional WACC range
BESS replacement unit cost, year 10	$c_{B,10}$	Normal	271 USD/kWh	$\sigma =$ 40USD/kWh	Way et al. learning-curve forecast [27]
PV degradation rate	δ_{PV}	Constant	0.5%/yr	—	Crystalline-silicon median per [31]
Grid emission factor	EF_{grid}	Constant	0.4999 $kgCO_2/kWh$	—	TGO 2024 [5]

All stochastic inputs are sampled independently except where physically coupled. The discount rate is truncated to 4–12% to exclude implausible values for Thai institutional weighted average cost of capital (WACC). The fleet-utilization multiplier, M_D, jointly scales both annual EV charging demand and the avoided-diesel benefit. Convergence of the mean NPV was verified using 5,000 scenarios, with the 95% confidence-interval half-width remaining below USD 700.

3. Results

3.1. Siting Decision: Two Distributed Stations vs. One Centralized Station

Table 6 compares two charging-infrastructure layouts for the revised 10-van electric shuttle fleet: one centralized station located at Huay Kaew (HK) and two distributed stations located at Huay Kaew and Doi Saket (HK + DS). The analysis follows the terminal-based fleet operation described in Section 2, where five vans are assigned to each terminal.

Table 6. Siting decision: one centralized station vs. two distributed stations.

Criterion	1 Station (HK only)	2 Stations (HK + DS)
Infrastructure CAPEX	113,857 USD	110,571 USD
PV capacity (total)	30 kWp (HK only)	60 kWp, 30 kWp × 2 stations
BESS capacity (total)	300 kWh	200 kWh, 100 kWh × 2 stations
Dead-run distance	47,600 km/year	0 km/year
Dead-run energy waste	8,901 kWh/year	0 kWh/year
Annual PV electricity-credit value	$2,764/yr	$5,528/yr
Annual net benefit	$42,057/yr	$45,966/yr
System NPV (r=8%, N=15)	$36,980	$86,293
BESS replacement cost, year 10	USD 81,429	USD 54,286
Present value of BESS replacement	USD 37,717	USD 25,145
ΔNPV (2-station advantage)	—	+$49,313
Verdict	NPV-dominated	NPV-dominant

In the centralized configuration, all vans are assumed to be charged at HK. Therefore, the five DS-based vans must travel empty from DS to HK after the final daily service trip and return empty to DS before the next operating day. This creates a dead-run distance of 280 km/day, or 47,600 km/year over 170 normal-semester operating days. Based on the EV energy consumption rate of 0.187 kWh/km, this corresponds to 8,901 kWh/year of additional non-revenue electricity demand.

The distributed configuration eliminates this dead-run operation because each fleet group is charged at its own terminal. As a result, the HK + DS configuration avoids unnecessary vehicle movement, reduces energy waste, and preserves the terminal-based fleet-rotation pattern. It also reduces operational complexity and avoids concentrating all charging activity at a single location.

 doi:10.20944/preprints202605.0703.v1

The siting decision also affects infrastructure sizing. In the centralized case, the HK station must supply both the normal fleet demand and the additional dead-run energy. The maximum daily charging demand therefore increases from 157.08 kWh/day to 209.44 kWh/day, requiring a practical BESS capacity of 300 kWh and three 7.4 kW Level-2 chargers. In contrast, the distributed configuration serves 78.54 kWh/day at each station and requires only 100 kWh BESS and one 7.4 kW charger per station. Thus, the total distributed system requires 200 kWh BESS and two chargers.

Economically, the two-station configuration is also preferable. The estimated infrastructure CAPEX is USD 110,571 for the distributed system, compared with USD 113,857 for the centralized system, giving an initial CAPEX saving of USD 3,286. The incremental value of the distributed configuration can be separated into two components. First, the siting-only benefit avoids 8,901 kWh/year of dead-run electricity consumption, equivalent to USD 1,144/year at an electricity tariff of USD 0.129/kWh. Second, the distributed rooftop-PV opportunity enables an additional 30 kWp PV system at DS, producing approximately 43,975 kWh/year with an annual internal electricity-credit or campus self-consumption value of USD 2,764 at 2.20 THB/kWh. Therefore, the total annual incremental benefit is USD 3,909/year, of which USD 1,144/year is attributable strictly to avoided dead-run energy.

Over a 15-year project lifetime at an 8% discount rate, the present value of the annual distributed-configuration benefit is approximately USD 33,457. When the initial CAPEX saving of USD 3,286 and the discounted year-10 BESS replacement-cost advantage of approximately USD 12,571 are included, the distributed configuration provides a total NPV advantage of approximately USD 49,313 (≈ THB 1.726 million at 1 USD = 35 THB). Therefore, the two-station HK + DS layout is selected as the baseline charging-infrastructure configuration for the subsequent PV–BESS sizing, KKT optimization, techno-economic analysis, and environmental assessment. These comparative results are illustrated in Figure 4.

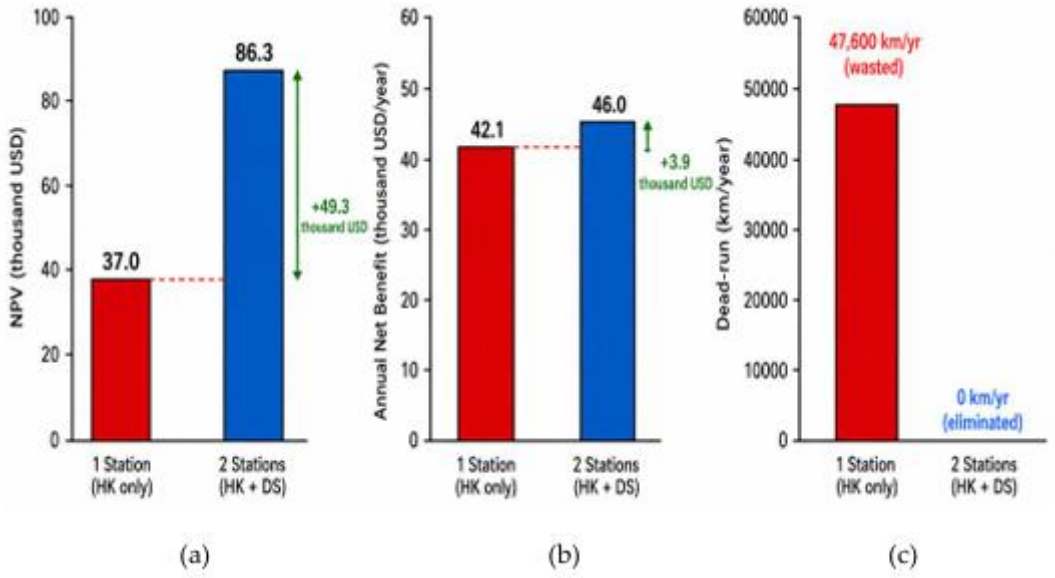

Figure 4. Siting decision comparison: one centralized station at Huay Kaew (HK only) versus two distributed stations at Huay Kaew and Doi Saket (HK + DS). (a) System NPV over 15 years at a discount rate of 8%; (b) annual net benefit in Year 1; and (c) annual dead-run distance eliminated. The two-station configuration provides an NPV advantage of USD 49,313 after including the year-10 BESS replacement cost and eliminates 47,600 km/year of unproductive dead-run travel.

3.2. Optimal System Configuration

Table 7 presents the complete optimal sizing results for the two distributed charging stations, with the analytical solution verified against the KKT closed-form derivation and Differential

 doi:10.20944/preprints202605.0703.v1

Evolution. The solution is a corner-point optimum located at the intersection of two binding constraints: g_7, the PV rooftop-area constraint, and g_4, the BESS one-day autonomy constraint. The PV constraint is active because the marginal NPV contribution of additional PV capacity remains positive throughout the feasible region ($\partial NPV / \partial P_{PV}$ ≈ +161 USD/kWp). Conversely, the BESS autonomy constraint is active because the full lifecycle marginal NPV contribution of additional storage capacity beyond the required one-day autonomy is negative. When the initial BESS CAPEX, the present value of the year-10 replacement liability, and incremental O&M are included, the marginal contribution is approximately $\frac{\partial NPV}{\partial E_{\mathrm{BESS}}} \approx -\left[c_B + \frac{c_B}{(1+r)^{10}} + c_B \rho_{\mathrm{OM}} A_N\right] \approx -441$ USD/kWh. This confirms that additional BESS capacity beyond the autonomy requirement reduces lifecycle value because it increases initial investment, replacement cost, and O&M without increasing scheduled EV charging demand.

Accordingly, the theoretical KKT solution gives $P^*_{PV} = 30$ kWp and $E^*_{BESS} = 94.85$ kWh per station, where $E^*_{BESS} = 78.54/(0.92 \times 0.90)$. For practical implementation, the theoretical BESS capacity is rounded up to a commercially available 100 kWh LFP module at each station. This rounding increases the total installed BESS capacity from the theoretical system optimum of 189.70 kWh to the practical system capacity of 200 kWh, corresponding to an additional 10.30 kWh of storage. At a unit BESS cost of USD 271/kWh, this represents a practical modular-sizing premium of approximately USD 2,796. This premium is considered acceptable because it arises from discrete commercial battery-module availability while preserving the KKT-derived design logic and ensuring adequate operational autonomy.

The marginal NPV gradients reported in Table 7 are evaluated at the corner-point optimum and use the following conventions: $\partial NPV / \partial P_{PV}$ ≈ +161 USD/kWp is computed from Eq. (56) using $H_{PSH} = 5.02$h/day, $PR = 0.80$, $v_{PV} = 0.0629$USD/kWh (2.20 THB/kWh), annuity factor $A_N = 8.5595$(15-year horizon at $r = 8\%$), and $c_{PV} = 629$ USD/kWp, yielding 365 × 5.02 × 0.80 × 0.0629 × 8.5595 − 629 ≈ +161 USD/kWp. The negative gradient $\partial NPV / \partial E_{\mathrm{BESS}} \approx -441$ USD/kWh is evaluated using $c_B = 271$ USD/kWh, $r = 8\%$, year-10 replacement, $\rho_{\mathrm{OM}} \approx 1.9\%$, and $A_N = 8.5595$. It includes the initial marginal BESS CAPEX, the discounted replacement liability $c_B(1 + r)^{-10}$, and the present value of incremental O&M $c_B \rho_{\mathrm{OM}} A_N$. Therefore, BESS capacity above the one-day autonomy boundary is economically undesirable in the deterministic model.

Table 7. Optimal PV-BESS configuration per station.

Parameter	Station HK	Station DS	System total	Constraint / status
KKT PV capacity, P^*_{PV}	30 kWp	30 kWp	60 kWp	g_7 active, rooftop-area limit
KKT BESS capacity, E^*_{BESS}	94.85 kWh	94.85 kWh	189.70 kWh	g_4 active, one-day autonomy
Practical BESS capacity	100 kWh	100 kWh	200 kWh	Commercial modular rounding
Usable BESS energy	82.80 kWh	82.80 kWh	165.60 kWh	$E_{\mathrm{usable}} > E_{\mathrm{max}}$
Charger rating	7.4 kW AC	7.4 kW AC	14.8 kW AC	g_5 inactive, charger adequate
Annual PV generation	43,975.2 kWh/yr	43,975.2 kWh/yr	87,950.4 kWh/yr	—
Annual EV charging demand	15,341.5 kWh/yr	13,351.8 kWh/yr	28,693.3 kWh/yr	—
Annual PV surplus	28,633.7 kWh/yr	30,623.4 kWh/yr	59,257.1 kWh/yr	Export / campus use
PV-to-demand ratio	286.6%	329.4%	306.5%	g_3 inactive, solar fraction satisfied

 doi:10.20944/preprints202605.0703.v1

LOLE	≈0 h/yr	≈0 h/yr	≈0 h/yr	g_1 inactive, reliability satisfied
Diesel-equivalent COE benchmark	34.51 THB/kWh	34.51 THB/kWh	34.51 THB/kWh	g_2 inactive, below benchmark
Station-level budget status	Below limit	Below limit	—	g_6 inactive

Overall, the KKT-based configuration demonstrates a clear engineering interpretation. The PV capacity is maximized at the rooftop-area constraint because additional PV generation provides positive economic value. Conversely, the BESS capacity is limited to the minimum one-day autonomy requirement because further storage expansion increases cost without increasing the scheduled shuttle energy demand. Thus, the optimal distributed charging infrastructure consists of 30 kWp PV and 100 kWh BESS per station, or 60 kWp PV and 200 kWh BESS at the system level. This configuration satisfies the energy sufficiency, autonomy, charger adequacy, and reliability constraints while generating a substantial annual PV surplus for campus use or export.

Accordingly, the optimal station-level configuration is located at the intersection of the PV rooftop-area constraint and the BESS one-day autonomy constraint, as shown in Figure 5. This graphical result confirms that g_4 and g_7 are the only binding constraints governing the optimal sizing solution. The NPV contours increase toward the PV upper bound, indicating that additional PV capacity has a positive marginal economic contribution. In contrast, BESS capacity above the minimum autonomy requirement increases system cost without increasing the scheduled EV charging demand. Thus, the theoretical KKT optimum is 30 kWp PV and 94.85 kWh BESS per station, which is rounded up to a practical 100 kWh BESS module for implementation.

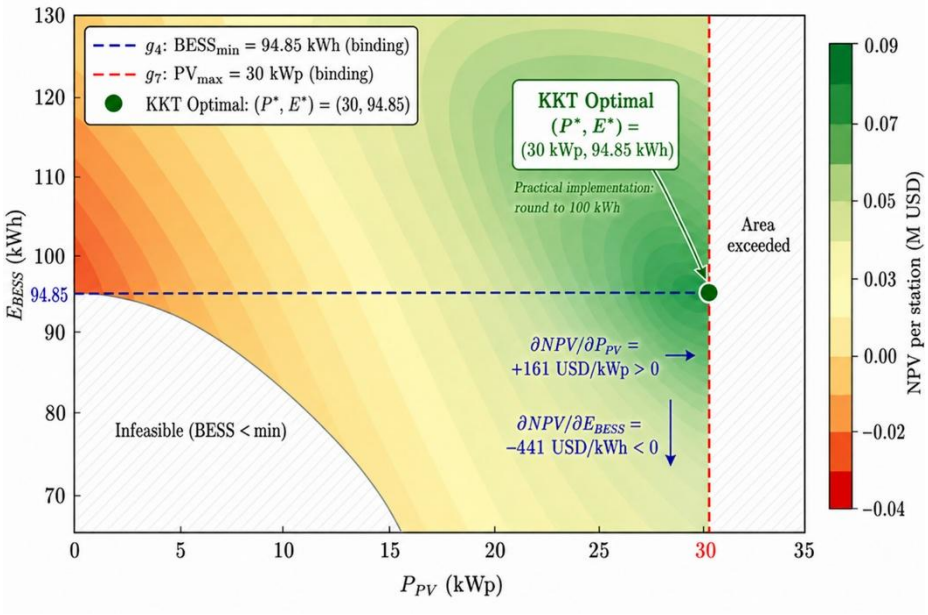

Figure 5. KKT feasible region and NPV contours for Station Huay Kaew.

3.3. Financial Performance

Table 8 presents the deterministic financial performance of the optimal two-station PV–BESS configuration over a 15-year project lifetime at an 8% discount rate (1 USD = 35 THB used for THB → USD conversion of input data). The model considers both charging-infrastructure investment and the incremental EV-shuttle-van acquisition cost. The infrastructure (60 kWp PV, 200 kWh LFP BESS, two 7.4 kW chargers) has a CAPEX of USD 110,571 (USD 110,571); the EV premium for 10 vans is USD 171,429 (USD 171,429); total incremental investment is USD 282,000. No direct EV 3.5 purchase

 doi:10.20944/preprints202605.0703.v1

subsidy is deducted from the base-case investment cost. This conservative treatment avoids overstating the project NPV, because subsidy eligibility depends on vehicle category, procurement conditions, battery capacity, local-production requirements, and the incentive rules in force at the time of procurement.

Annual benefits derive from three sources: avoided diesel cost (USD 28,292/year, 61.6%), reduced maintenance (USD 12,143/year, 26.4%), and PV electricity value at USD 0.0629/kWh (2.20 THB/kWh) (USD 5,528/year, 12.0%), totaling USD 45,966/year. The PV electricity value is not treated as a guaranteed feed-in tariff. Instead, it is modelled as an internal campus electricity-credit or self-consumption value. To test this assumption, the financial model also evaluates conservative credit scenarios. If the PV credit is discontinued after year 5, the project NPV decreases from USD 86,293 to approximately USD 61,048. If no PV surplus credit is assigned over the project lifetime, the NPV remains positive at approximately USD 38,973. Therefore, the investment conclusion does not depend solely on PV-credit revenue.

On a full-transition basis, the proposed EV + PV–BESS system achieves a net present value of USD 86,293 over the 15-year project period. The internal rate of return is approximately 12.9%, which is substantially higher than the assumed discount rate of 8%. The simple payback period is 6.1 years when both the charging infrastructure and the incremental electric-shuttle-van acquisition cost are included. The discounted payback period is approximately 8.8 years. If the charging infrastructure is evaluated separately from the incremental acquisition cost of the electric shuttle vans, the simple payback period decreases to approximately 2.4 years, indicating that the PV–BESS infrastructure itself is financially strong and that the longer full-transition payback is mainly attributable to the incremental acquisition cost of the electric shuttle vans.

Table 8. Techno-economic performance summary of the optimal two-station PV–BESS charging system ($r = 8\%$, $N = 15$ years, 1 USD = 35 THB).

Metric	Value (USD)	Note
Charging infrastructure CAPEX	USD 110,571	THB 3.870 million
Incremental electric-shuttle-van acquisition cost	USD 171,429	THB 6.000 million
BESS replacement cost, year 10	USD 54,286	200 kWh × 9,500 THB/kWh
Present value of BESS replacement	USD 25,145	Discounted at 8% for 10 years
Total incremental CAPEX	USD 282,000	Infrastructure + incremental vehicle acquisition cost
Annual diesel fuel saving	USD 28,292/year	Based on 20,459 L/year diesel avoidance
Annual O&M saving	USD 12,143/year	Lower EV maintenance cost
Annual PV electricity value	USD 5,528/year	87,950.4 kWh/year at 2.20 THB/kWh
Net annual benefit	USD 45,966/year	Fuel saving + O&M saving + PV value
NPV, full-transition basis	USD 86,293	15-year project lifetime
IRR, full-transition basis	12.9%	Higher than 8% discount rate
Simple payback, full transition	6.1 years	Based on total incremental CAPEX
Discounted payback, full transition	8.8 years	Based on 8% discount rate
Simple payback, infrastructure only	2.4 years	Excluding incremental vehicle acquisition cost

The benefit structure is not concentrated on a single revenue source: avoided diesel cost dominates and is largely independent of feed-in tariff policy or electricity-credit assumptions, making the project resilient to PV policy changes.

Table 9 extends the assessment to a Total Cost of Ownership (TCO) comparison. Although the diesel fleet has lower vehicle CAPEX, it incurs higher recurring fuel and maintenance expenses. The present-value TCO is USD 617,470 for the diesel baseline and USD 531,194 for EV + PV–BESS, giving a lifecycle saving of USD 86,276—consistent with the deterministic NPV within rounding.

 doi:10.20944/preprints202605.0703.v1

Table 9. Total Cost of Ownership (TCO) comparison: ICE diesel vs. EV + PV–BESS (15-year NPV basis, r = 8%).

Cost / Benefit Item	Diesel baseline	EV + PV–BESS	EV Advantage
Vehicle purchase, 10 vans	USD 228,571	USD 400,000	−USD 171,429
Present value of BESS replacement	—	USD 25,145	−USD 25,145
Charging infrastructure CAPEX	—	USD 110,571	−USD 110,571
Present value of diesel fuel cost	USD 242,164	—	+USD 242,164
Present value of scheduled O&M cost	USD 146,734	USD 42,798	+USD 103,936
Present value of PV electricity credit	—	−USD 47,320	+USD 47,320
Total 15-year TCO	USD 617,470	USD 531,194	+USD 86,276
TCO per kilometer	USD 0.268/km	USD 0.231/km	14.0% reduction

The TCO comparison confirms that the higher EV + PV–BESS initial investment is recovered through lower operating expenditure: lifecycle cost decreases from USD 0.268/km to USD 0.231/km (14.0% reduction). The cumulative cash-flow profile is shown in Figure 6.

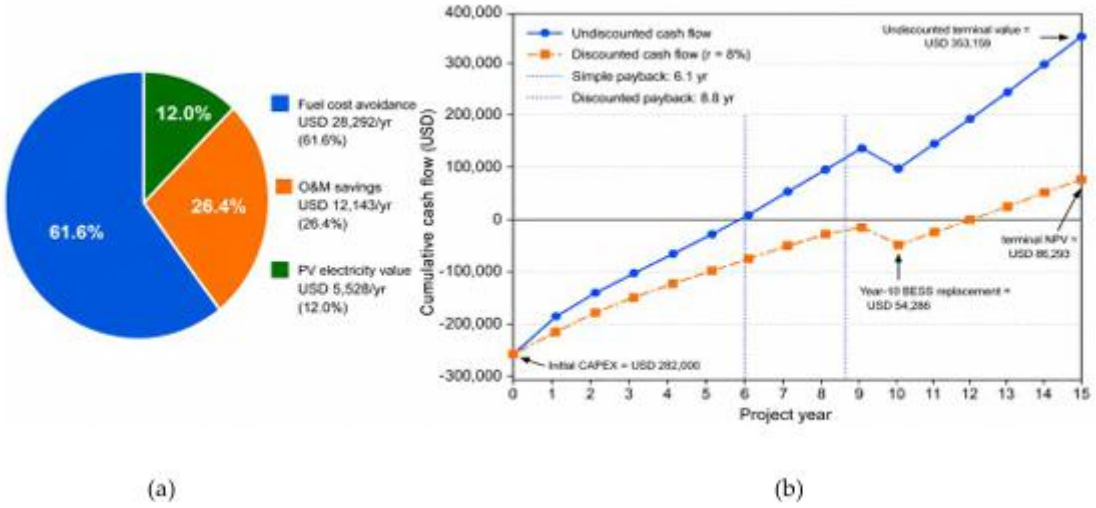

Figure 6. Financial performance overview of the optimal two-station EV + PV–BESS configuration. (a) Annual benefit breakdown, including fuel cost avoidance (61.6%, USD 28,292 yr^{-1}), O&M savings (26.4%, USD 12,143 yr^{-1}), and PV electricity value from campus self-consumption or internal electricity credit (12.0%, USD 5,528 yr^{-1}), giving a total annual benefit of USD 45,966 yr^{-1}. (b) Cumulative undiscounted and discounted cash-flow profiles over the 15-year project lifetime on a full-transition CAPEX basis, including both charging-infrastructure investment and the incremental electric-shuttle-van acquisition cost. The simple payback period is 6.1 years, the discounted payback period is 8.8 years, and the terminal NPV is USD 86,293.

3.4. Environmental Impact

The environmental impact of the proposed EV + PV–BESS transition was assessed across three scenarios: the diesel baseline, a grid-charged EV scenario, and the optimal EV + PV–BESS configuration. The diesel baseline was based on the 10-van fleet's annual fuel consumption; the EV scenarios used the annual charging demand from the energy-consumption model. Emission factors were 3.147 $kgCO_2/L$ for diesel (well-to-wheel), 0.4999 $kgCO_2/kWh$ for the Thai grid (TGO 2024), and 0.020 $kgCO_2/kWh$ for PV electricity (IEA PVPS Task 12 [31]).

The annual emission reduction was calculated as

$$\Delta CO_2 = L_{diesel} EF_{diesel} - E_{EV}\left[f_{sol} EF_{PV} + (1 - f_{sol}) EF_{grid}\right] \quad (99)$$

 doi:10.20944/preprints202605.0703.v1

where L_{diesel} is the annual diesel consumption, EF_{diesel} is the diesel emission factor, E_{EV} is the annual EV charging demand, f_{sol} is the effective solar fraction, EF_{PV} is the lifecycle PV emission factor, and EF_{grid} is the grid emission factor.

The diesel baseline (20,459 L/year) produces ≈64.39 tCO_2/year. Grid-only EV charging (28,693.3 kWh/year × 0.4999 $kgCO_2$/kWh) produces ≈14.34 tCO_2/year, a 77.7% reduction from electrification alone.

For the EV + PV–BESS configuration, an effective solar fraction of 85% was adopted for conservative environmental accounting; the remaining 15% is assumed to be grid backup. This blended supply gives an effective emission factor of 0.0920 $kgCO_2$/kWh and annual EV-charging emissions of 2.64 tCO_2/year, a 95.9% reduction relative to the diesel baseline (Table 10). Although annual PV generation exceeds the EV demand, the conservative 85% solar fraction avoids over-crediting surplus PV electricity and reflects the temporal mismatch between PV generation, BESS operation, and charging demand.

Table 10. CO_2 emission comparison across diesel, grid-EV, and EV + PV–BESS scenarios.

Scenario	Annual CO_2 emissions	Reduction	15-yr total
Diesel baseline	64.39 tCO_2/yr	—	965.9tCO_2
EV + 100% grid	14.34 tCO_2/yr	−77.7%	215.2tCO_2
EV + 85% solar (optimal)	2.64 tCO_2/yr	−95.9%	39.6tCO_2
CO_2 saved (EV solar vs. diesel)	61.75 tCO_2/yr	95.9%	926.3tCO_2

The CO_2 scenario analysis shows that most of the emission reduction comes from the ICE-to-EV transition; the PV–BESS system contributes additional reduction by displacing grid electricity with low-carbon solar electricity. Over the 15-year lifetime, the optimal configuration avoids ≈926.3 tCO_2. This supports Thailand's Nationally Determined Contribution target of 30–40% GHG reduction by 2030.

Embodied carbon of the PV and BESS components was evaluated through the carbon payback period (CPBP):

$$CPBP = \frac{C_{embodied}}{\Delta CO_{2,annual}} = \frac{C_{PV,embodied} + C_{BESS,embodied}}{\Delta CO_{2,annual}} \quad (100)$$

The 60 kWp PV system contributes 36.0 tCO_2 (600 $kgCO_2$/kWp, after Frischknecht et al. [31]); the 200 kWh LFP BESS contributes 15.0 tCO_2 (75 $kgCO_2$/kWh, after Emilsson and Dahllöf [43]), giving a total of 51.0 tCO_2 (Table 11).

Table 11. Carbon payback period of the PV–BESS infrastructure.

Component / Metric	Capacity	Emission factor	Carbon value
PV system	60 kWp	600 $kgCO_2$/kWp	36.0 tCO_2
Initial LFP BESS	200 kWh	75 $kgCO_2$/kWh	15.0 tCO_2
Initial PV–BESS embodied carbon	—	—	51.0 tCO_2
Annual CO_2 reduction vs. diesel baseline	—	—	61.75 tCO_2/year
Initial carbon payback period	—	—	0.83 year
Year-10 replacement LFP BESS	200 kWh	75 $kgCO_2$/kWh	15.0 tCO_2
Lifecycle PV–BESS embodied carbon including replacement	—	—	66.0 tCO_2
Adjusted carbon payback period including replacement	—	—	1.07 years

 doi:10.20944/preprints202605.0703.v1

Against the annual reduction of 61.75 tCO_2/year, the initial CPBP is 0.83 years. Including the year-10 BESS replacement (+15.0 tCO_2) raises the lifecycle embodied carbon to 66.0 tCO_2, giving an adjusted CPBP of 1.07 years. Both values are substantially shorter than the financial payback period (Section 3.3). The carbon payback boundary excludes vehicle-manufacturing embodied emissions. The annual reduction and CPBP are illustrated in Figure 7.

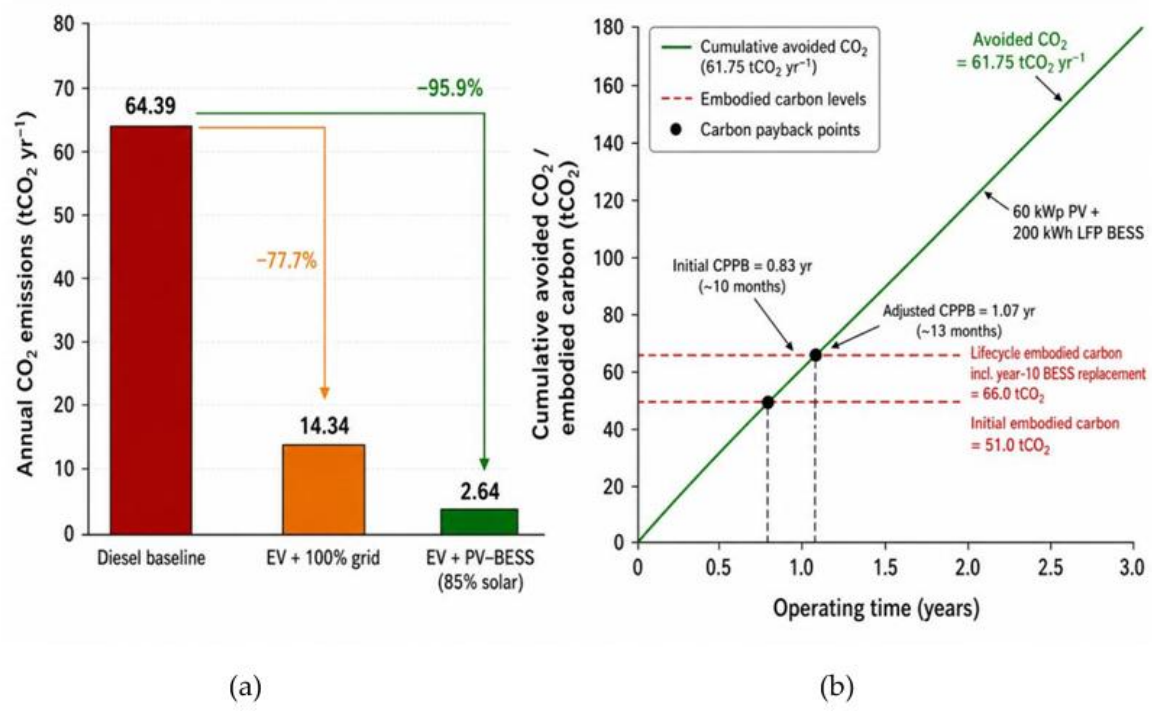

Figure 7. CO_2 emission comparison and carbon payback of the optimal EV + PV–BESS configuration. (a) The EV + PV–BESS system reduces annual CO_2 emissions from 64.39 to 2.64 tCO_2 $year^{-1}$, equivalent to a 95.9% reduction relative to the diesel baseline. (b) The initial PV–BESS embodied carbon of 51.0 tCO_2 is offset within 0.83 years. Including the year-10 BESS replacement increases the lifecycle embodied carbon to 66.0 tCO_2, giving an adjusted carbon payback period of 1.07 years.

Operational CO_2 sensitivity to future Thai grid decarbonization was also evaluated (Table 12). As the grid emission factor decreases, the EV + PV–BESS effective blended factor decreases from 0.0920 $kgCO_2$/kWh under the current grid to 0.0395 $kgCO_2$/kWh under a long-term low-carbon scenario (0.1500 $kgCO_2$/kWh), and annual EV + PV–BESS emissions decrease from 2.64 to 1.13 tCO_2/year.

Table 12. CO_2 reduction sensitivity to Thai Grid Emission Factor (GEF) decarbonization trajectory.

Year / Scenario	GEF ($kgCO_2$/kWh)	Blended EF, EV + PV–BESS ($kgCO_2$/kWh)	EV + PV–BESS CO_2 (tCO_2/yr)	Reduction vs. diesel	15-yr CO_2 avoided (tCO_2)
2024 current grid	0.4999	0.0920	2.64	95.9%	926.3
2027 NDC progress	0.4200	0.0800	2.30	96.4%	931.4
2030 NDC target	0.3500	0.0695	1.99	96.9%	935.9
2035 deep decarbonization	0.2500	0.0545	1.56	97.6%	942.4
2040 long-term low-carbon grid	0.1500	0.0395	1.13	98.2%	948.8

 doi:10.20944/preprints202605.0703.v1

The blended emission factor for the EV + PV–BESS scenario is calculated as $EF_{\text{blend}} = 0.85EF_{\text{solar}} + 0.15GEF$, where $EF_{\text{solar}} = 0.020$ kgCO₂/kWh and GEF is the Thailand grid emission factor. The diesel baseline is 64.39 tCO₂/year, calculated from 20,459 L/year of diesel consumption and a well-to-wheel diesel emission factor of 3.147 kgCO₂/L. The values in Table 12 represent operational CO_2 emissions only; embodied emissions from the PV–BESS infrastructure and the year-10 BESS replacement are evaluated separately in Table 11 and Figure 7. The GEF trajectory is based on Thailand's National Energy Plan and Nationally Determined Contribution pathway, while the 2035–2040 values are treated as scenario estimates. As the Thai grid decarbonizes, the residual grid-backup component of the EV + PV–BESS system becomes progressively cleaner, reducing annual operational emissions from 2.64 tCO₂/year under the current grid factor to 1.13 tCO₂/year under the long-term low-carbon grid scenario. This confirms that the environmental advantage of the proposed EV + PV–BESS transition strengthens over time as renewable energy penetration increases [32,33]. The combined economic and environmental payback behavior, together with the CO_2 reduction sensitivity to future Thai grid decarbonization, is illustrated in Figure 8.

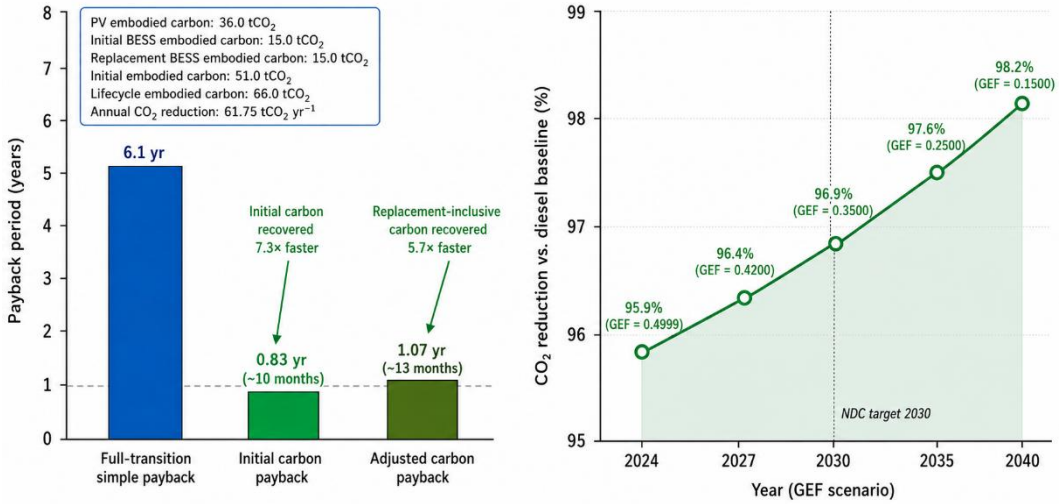

(a) **(b)**

Figure 8. ICE-to-EV transition: economic versus environmental payback and grid-emission-factor sensitivity. (a) The full-transition simple payback period is 6.1 years, while the initial CPBP is 0.83 years. Including the year-10 BESS replacement increases the adjusted CPBP to 1.07 years; therefore, the environmental payback remains about 5.7–7.3 times faster than the financial payback. (b) The CO_2 reduction remains above 95.9% under the current grid condition and improves to 98.2% under the long-term low-carbon grid scenario with GEF = 0.15 kgCO₂/kWh.

3.5. Stochastic Risk Analysis

Monte Carlo simulation with 5,000 scenarios was conducted to evaluate the financial robustness of the optimal two-station EV + PV–BESS configuration under techno-economic uncertainty. The stochastic model accounts for uncertainty in diesel price, fuel-price escalation, solar resource, fleet utilization, PV electricity-credit value, O&M cost, and discount rate. The resulting NPV distribution is shown in Figure 9, and the corresponding risk metrics are summarized in Table 13.

After including the year-10 BESS replacement cost, the simulated NPV distribution remains positive across the adopted uncertainty range. The probability of positive NPV is $P(NPV > 0) = 100\%$ within the 5,000-scenario set. The mean NPV is approximately USD 64,158, with a median of USD 61,834. The standard deviation is approximately USD 24,285 and the coefficient of variation is 37.9%; the replacement cost reduces the expected NPV while leaving the main uncertainty spread largely unchanged. The 5th-percentile value-at-risk is $VaR_5\%$ ≈ USD 28,959 indicating that the project remains financially viable even under adverse combinations of diesel price, fuel escalation, solar

 doi:10.20944/preprints202605.0703.v1

resource, fleet utilization, PV electricity-credit value, O&M cost, and discount rate. The conditional value-at-risk is $CVaR_5\%$ ≈ USD 21,248 [30], confirming that the downside tail remains positive after accounting for battery replacement.

These stochastic results support the deterministic financial conclusion reported in Section 3.3. Although the year-10 BESS replacement reduces the mean NPV relative to the no-replacement case, the project remains financially robust because the economic value is primarily driven by avoided diesel fuel cost, reduced vehicle maintenance, and PV electricity value. Diesel price volatility and discount rate remain the dominant financial risk factors, as further examined in the tornado sensitivity analysis in Figure 10.

Table 13. Stochastic NPV risk metrics based on 5,000 Monte Carlo scenarios.

Risk metric	Revised value	Interpretation
Mean NPV	USD 64,158	Expected lifecycle return after year-10 BESS replacement
Median NPV	USD 61,834	Central tendency of simulated NPV distribution
Standard deviation	USD 24,285	Moderate dispersion under techno-economic uncertainty
Coefficient of variation	37.9%	Relative NPV uncertainty after replacement cost is included
$\boldsymbol{P(\mathrm{NPV} > 0)}$	=100% within 5,000 scenarios set	No loss-making case was observed under the adopted uncertainty ranges.
$\boldsymbol{P(\mathrm{NPV} > 50{,}000)}$	≈ 72.0%	Probability of maintaining a strong positive NPV after replacement
$\boldsymbol{VaR_{5\%}}$	USD 28,959	5th-percentile downside threshold
$\boldsymbol{CVaR_{5\%}}$	USD 21,248	Expected NPV in the worst 5% of scenarios

The left tail represents adverse techno-economic outcomes arising from combined variations in diesel price, fuel-price escalation, solar resource, fleet utilization, PV electricity-credit value, O&M cost, and discount rate. After including the scheduled year-10 BESS replacement cost, the 5th-percentile value-at-risk decreases to approximately USD 28,959 while the conditional value-at-risk remains positive at approximately USD 21,248. This indicates that the project remains financially viable even under adverse parameter combinations.

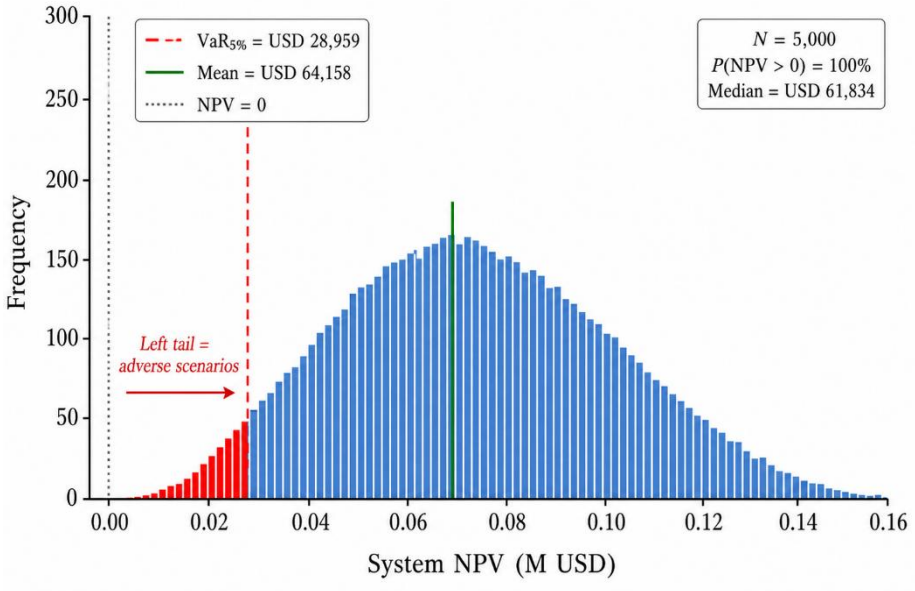

Figure 9. Monte Carlo NPV distribution based on 5,000 scenarios.

 doi:10.20944/preprints202605.0703.v1

3.6. Deterministic Stress-Scenario Analysis

Although the 5,000-scenario Monte Carlo simulation yields $P(NPV > 0) = 100\%$ within the adopted uncertainty ranges, this result is conditional on the adopted input distributions. To stress-test the deterministic design beyond the central tendency of those distributions, five deterministic stress scenarios, including four adverse cases and one favorable case, were evaluated. Table 14 reports the resulting NPV for each scenario.

Table 14. Deterministic stress-scenario NPV under joint techno-economic parameter movements.

Scenario	Initial diesel price, $p_{d,0}$	Daily PSH, H_{PSH}	Discount rate, r(%)	Diesel escalation rate, g_d	NPV (USD)	Interpretation
Base case	1.383 USD/L	5.02 h/day	8.0%	3.0%/yr	86,293	Reference
S1: Diesel-price collapse	0.80 USD/L	5.02 h/day	8.0%	1.5%/yr	≈ −15,800	Negative NPV
S2: Solar shortfall	1.383 USD/L	4.00 h/day	8.0%	3.0%/yr	≈ +76,700	Robust
S3: High discount rate + low diesel price	1.10 USD/L	5.02 h/day	12.0%	1.5%/yr	≈ −25,800	Negative NPV
S4: Combined adverse	0.90 USD/L	4.30 h/day	11.0%	1.0%/yr	≈ −47,300	Significantly negative
S5: Favorable	1.66 USD/L	5.50 h/day	6.0%	4.5%/yr	≈ +194,300	Strong upside

Scenarios S1, S3, and S4 demonstrate that the project is not unconditionally robust: a sustained diesel-price collapse to USD 0.80–0.90/L (e.g., S1 NPV ≈ −USD 15,800) (≈ 28–32 THB/L), in isolation or combined with high discount rates (S3 NPV ≈ −USD 25,800), or simultaneous adverse parameter movement (S4 NPV ≈ −USD 47,300), can drive NPV negative. These adverse states fall outside the central Monte Carlo distribution but should be considered as low-probability tail risks. The principal sensitivity, as confirmed by the tornado analysis in Section 3.7, is to diesel price, reflecting the dominant role of fuel-cost avoidance (61.6%) in the annual benefit structure. Mitigation via long-term diesel-price hedging, structured PPAs for the PV credit, or institutional carbon-pricing internalization should be considered at deployment time.

3.7. Sensitivity (Tornado) Analysis

A one-way sensitivity analysis was conducted to identify the dominant techno-economic parameters affecting the system-level NPV after including the scheduled year-10 BESS replacement cost. Each parameter was perturbed individually around its base-case value, while all other parameters were held constant. The base-case NPV used in the sensitivity analysis is USD 86,293, consistent with the deterministic financial result reported in Section 3.3. The resulting NPV responses are summarized in Table 15 and visualized as a tornado chart in Figure 10.

The results show that diesel price and discount rate are the two dominant uncertainty drivers. A ±20% change in diesel price produces the largest NPV swing, from USD 37,841 under the adverse case to USD 134,707 under the favorable case. This confirms that the project value is strongly governed by avoided diesel fuel consumption. The discount rate is the second most influential parameter, with NPV varying from USD 46,670 under the adverse case to USD 134,087 under the favorable case. Unlike the other parameters, the discount-rate sensitivity also affects the present value of the year-10 BESS replacement cost; therefore, the replacement liability is discounted using the corresponding perturbed discount rate.

Fuel-price escalation and PV electricity-credit value have secondary effects, while solar-resource variability and fleet-utilization uncertainty have smaller impacts. BESS capacity is excluded from the tornado analysis because it is analytically fixed by the binding KKT autonomy constraint and therefore does not represent an independent sensitivity variable beyond the minimum feasible storage requirement. Overall, the sensitivity results confirm that the EV + PV–BESS transition remains

 doi:10.20944/preprints202605.0703.v1

NPV-positive across all tested one-way adverse cases after accounting for the year-10 BESS replacement cost.

Table 15. Tornado sensitivity analysis: NPV response to one-way parameter perturbation.

Parameter	Perturbation	NPV under adverse case	NPV under favorable case	NPV swing
Diesel price	±20%	USD 37,841	USD 134,707	USD 96,866
Discount rate	±2%	USD 46,670	USD 134,087	USD 87,417
Fuel escalation rate	±1.5%	USD 73,097	USD 99,489	USD 26,392
PV electricity-credit value	±0.50 THB/kWh	USD 75,520	USD 97,029	USD 21,509
Solar resource, PSH	±17%	USD 78,230	USD 94,318	USD 16,088
Fleet utilization / EV demand	±15%	USD 83,570	USD 89,016	USD 5,446

Figure 10 presents the tornado sensitivity analysis of system-level NPV under one-way parameter perturbations after including the year-10 BESS replacement cost. The results indicate that diesel price and discount rate are the dominant financial risk drivers. Diesel price directly affects the value of avoided fuel consumption, while the discount rate affects both the present value of future benefits and the discounted replacement cost. PV electricity-credit value and solar-resource uncertainty have more moderate effects, whereas fleet-utilization uncertainty has the smallest impact within the adopted perturbation range. BESS capacity is excluded from the tornado analysis because it is analytically fixed by the binding KKT autonomy constraint, g_4, and therefore does not represent an independent design variable beyond the minimum feasible storage requirement.

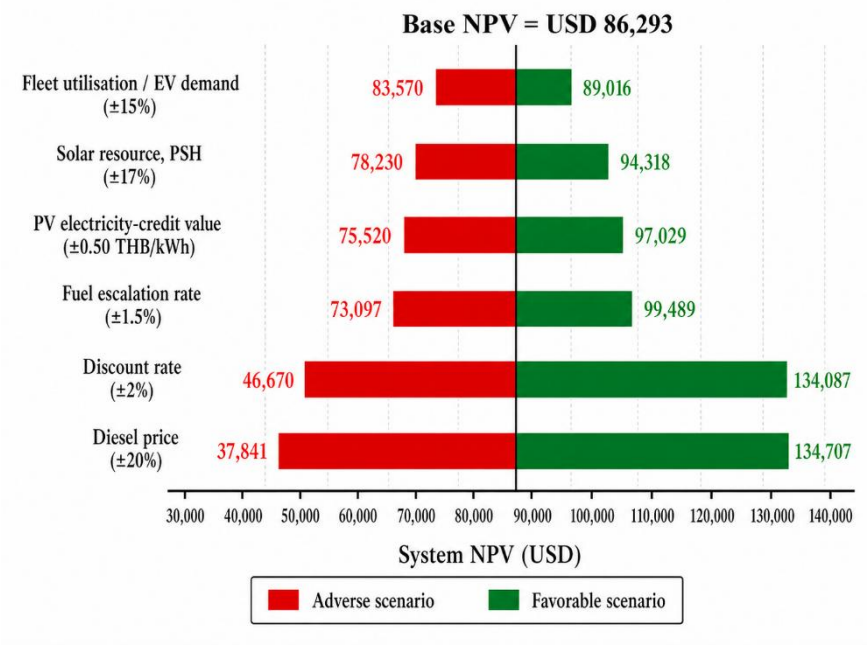

Figure 10. Tornado sensitivity analysis of system NPV.

Each bar shows the change in system-level NPV when one parameter is varied across its plausible range while all other parameters are held at their base-case values. The base-case NPV is USD 86,293. Diesel price and discount rate are the dominant financial risk drivers. Green bars indicate favorable parameter movement, while red bars indicate adverse parameter movement

 doi:10.20944/preprints202605.0703.v1

3.8. Exchange-Rate Sensitivity

The base-case analysis adopts a fixed exchange rate of 35 THB/USD. Both CAPEX (PV modules, BESS cells, inverters, all USD-denominated imports) and the diesel-cost term in the annual benefit are exchange-rate exposed, but they move in the same direction (a stronger THB reduces both equipment import cost and diesel cost), partially offsetting each other. Table 16 presents NPV under exchange-rate movements of ±10%.

Table 16. Exchange-rate sensitivity of system NPV (15-year horizon, r = 8%).

FX (THB/USD)	CAPEX adj.	Diesel-price adj.	Net NPV impact	NPV (USD)
32 (THB strong)	−8.6%	−8.6%	Slight increase	≈ 92,400
35 (Base)	0	0	—	86,293
38 (THB weak)	+8.6%	+8.6%	Slight decrease	≈ 80,600

A ±10% FX swing produces an NPV change of approximately ±USD 6,000 (≈ 7% of base NPV), markedly smaller than the diesel-price sensitivity reported in the tornado analysis. Both CAPEX and diesel cost are USD-correlated, providing a partial natural hedge against currency volatility.

4. Discussion

4.1. Significance of the KKT-Based Corner-Point Optimality Interpretation

The analytical framework in this study provides more than a numerical sizing result; it establishes an active-constraint interpretation of the revised seven-constraint PV–BESS sizing problem and explains why the optimum is located at a physically meaningful boundary solution. Conventional EV charging-station planning and sizing studies commonly rely on numerical optimization or metaheuristic search methods to identify feasible solutions [10–12,15,34–39]. Although methods such as Genetic Algorithm, Particle Swarm Optimization, and Differential Evolution can converge to high-quality solutions, they do not inherently explain which physical or economic constraints govern the optimum. In contrast, the KKT formulation identifies the active constraints directly and provides an analytical explanation for the resulting design. Under the verified monotonic objective structure and monotonic feasible design structure, the KKT conditions confirm that only two constraints are binding at the optimum: the BESS one-day autonomy constraint, g_4, and the PV rooftop-area constraint, g_7. The remaining constraints—LOLE reliability, COE competitiveness, minimum solar fraction, charger adequacy, and budget—are satisfied with positive slack and therefore do not determine the final sizing.

The economic interpretation is straightforward. Additional BESS capacity reduces NPV not only through CAPEX but also replacement liability, because replacement cost scales with installed BESS capacity. In this study, the installed LFP battery cost is represented by $C_{BESS} = \text{THB } 9{,}500/\text{kWh}$, based on the adopted 2024–2025 LFP market-price assumption. Therefore, once the autonomy boundary is satisfied, increasing E_{BESS} reduces NPV because the added storage capacity contributes cost but no additional operational revenue. Conversely, additional PV capacity remains economically beneficial within the feasible range because the generated electricity can offset EV charging energy, support campus self-consumption, or receive an internal electricity-credit value. As a result, the PV capacity is driven to the rooftop-area upper bound, while BESS capacity is driven to the minimum feasible autonomy boundary.

This leads to a simple and physically interpretable sizing rule. For each station, the optimal PV capacity is $P_{PV}^{*} = P_{PV,\max} = 30$ kWp, while the theoretical BESS requirement is $E_{BESS}^{*} = E_{\max}/(\eta_{BESS} DOD) = 94.85$kWh. For implementation, this theoretical value is rounded up to a commercially practical 100 kWh LFP module. Thus, the monotonic boundary argument combined with KKT active-constraint analysis converts the PV–BESS sizing problem from a purely numerical optimization exercise into a transparent engineering rule: maximize PV up to the available rooftop limit and size BESS only to the required one-day autonomy. The geometric interpretation in Figure 5

 doi:10.20944/preprints202605.0703.v1

supports this result, showing that the optimum occurs at the corner of the feasible region where g_4 and g_7 intersect, consistent with the closed-form KKT solution and the Differential Evolution verification.

4.2. Academic Calendar Operating Model

The academic-calendar operating model substantially affects the annual energy balance and economic interpretation of the proposed EV + PV–BESS system. If the normal-semester daily charging demand of 157.08 kWh/day were naively extended to a continuous 365-day operating year, the annual EV charging demand would be 57,334.2 kWh/year. In contrast, the calendar-aware model, which accounts for 170 normal-semester days and 38 reduced summer-semester days, gives a corrected annual EV charging demand of 28,693.3 kWh/year. Therefore, the actual annual demand is approximately 50.0% lower than the continuous-operation baseline; conversely, the 365-day assumption would overestimate EV energy demand by approximately 99.8%.

This correction has two important implications. First, because the 60 kWp PV system generates electricity throughout the full year, while the shuttle fleet operates according to the academic schedule, the system produces a substantial annual PV surplus. The total PV generation is 87,950.4 kWh/year, whereas the EV charging demand is only 28,693.3 kWh/year, resulting in 59,257.1 kWh/year of surplus PV electricity. This surplus can be exported to the campus grid, consumed by nearby institutional loads, or credited through an internal electricity-valuation mechanism, thereby improving the overall economic performance of the PV–BESS infrastructure.

Second, the academic calendar reduces annual energy throughput but does not reduce the required BESS autonomy capacity, because storage sizing is governed by the maximum daily station-level demand rather than the annual average demand. During normal-semester operation, each station must still support a peak daily charging requirement of 78.54 kWh/day. Consequently, the KKT-derived BESS requirement remains $E_{BESS}^{*} = 94.85$ kWh per station and is rounded up to a practical 100 kWh LFP module [25]. This finding highlights the importance of distinguishing between annual energy demand, which governs economic performance and PV surplus, and peak daily charging demand, which governs BESS sizing. Institutional fleet models that ignore academic or seasonal non-operating periods may therefore misrepresent annual utilization, PV surplus, and financial performance, even when the storage autonomy constraint remains controlled by the peak operating day.

4.3. Comparison with Prior Literature

Table 17 compares the proposed framework with six recent peer-reviewed studies on PV–BESS EV charging station optimization published between 2022 and 2025. The comparison focuses on four methodological dimensions that are directly relevant to this study: closed-form analytical sizing, optimality/verification approach, stochastic NPV risk assessment, and integrated CO_2/carbon analysis. These criteria were selected to distinguish between studies that provide only numerical sizing results and those that also offer analytical interpretability, investment-risk quantification, and environmental-performance evaluation.

Table 17. Methodological comparison with recent PV–BESS EV charging station optimization studies.

Study	Year	Method	Closed-form analytical solution	Optimality / verification approach	Stochastic NPV risk analysis	CO_2 /carbon analysis
Wei et al. [34]	2022	ANN-based data-driven sizing + Monte Carlo	✗	✗ Data-driven model	✓ Monte Carlo-based sizing uncertainty	✗
Sun et al. [35]	2022	Nonlinear programming for location and	✗	✗ Numerical NLP solution	✗	✓ Economic and

 doi:10.20944/preprints202605.0703.v1

		capacity optimization				environmental analysis
Dong et al. [36]	2024	MILP capacity and scheduling co-optimization	✗	✓ MILP optimality within the formulated model	✗	✗
Nafeh et al. [37]	2024	Modified Snake Optimization metaheuristic	✗	✗ Heuristic convergence	✗	✗
Gönül et al. [38]	2024	NSGA-II + TOPSIS multi-objective optimization	✗	✓ Pareto-front decision framework	✗	✓ CO_2 included in objective evaluation
Kassem et al. [39]	2025	HOMER-based PV/grid EV charging station simulation	✗	✗ Simulation-based search	✗	✓ Partial lifecycle/environmental assessment
This work	2026	KKT analytical sizing + DE verification + Monte Carlo NPV analysis	✓ $E^*_{BESS} = E_{\max}/(\eta_{BESS} DOD)$, $P^*_{PV} = P_{PV,\max}$	✓ Monotonic-boundary optimum under stated assumptions + DE numerical verification	✓ $N = 5{,}000$, $VaR_{5\%}$ of USD 28,959 and $CVaR_{5\%}$ of USD 21,248	✓ TCO, CPBP, and GEF sensitivity

Three observations emerge from Table 17. First, the closed-form analytical solution is the principal methodological contribution of this study. While MILP, nonlinear programming, multi-objective optimization, metaheuristics, and HOMER-based simulations can identify feasible or optimal numerical solutions, they do not usually provide simple closed-form engineering design rules. In contrast, the proposed KKT framework expresses the optimal BESS and PV capacities as explicit functions of daily energy demand, BESS efficiency, depth of discharge, and rooftop-area availability. For the revised RMUTL shuttle case, this gives $E^*_{BESS} = 94.85$ kWh and $P^*_{PV} = 30$ kWp per station, corresponding to a practical system design of 60 kWp PV and 200 kWh BESS for the two distributed stations.

Second, this study integrates deterministic optimal sizing with stochastic investment-risk analysis. The Monte Carlo simulation with 5,000 scenarios quantifies the downside risk of the fixed KKT-derived design under uncertainty in diesel price, fuel escalation, solar resource, fleet utilization, PV electricity-credit value, O&M cost, and discount rate. The resulting $VaR_{5\%}$ of USD 28,959 and $CVaR_{5\%}$ of USD 21,248 indicate that the project remains financially viable even under adverse parameter combinations after including the year-10 BESS replacement cost. This complements the deterministic financial result, where the full-transition case achieves NPV = USD 86,293, IRR = 12.9%, and a simple payback period of 6.1 years.

Third, the environmental assessment extends beyond annual operational CO_2 savings by including carbon payback and grid-emission-factor sensitivity. The proposed EV + PV–BESS configuration reduces annual emissions from 64.39 $tCO_2\ yr^{-1}$ for the diesel baseline to 2.64 $tCO_2\ yr^{-1}$ under the conservative 85% solar-charging assumption. The embodied carbon of the 60 kWp PV and 200 kWh LFP BESS system is recovered within approximately 0.83 years. When the year-10 BESS replacement is included, the adjusted carbon payback period increases to 1.07 years, which remains substantially shorter than the financial payback period.

A remaining distinction is the treatment of multi-period dispatch. Dong et al. [36] explicitly formulate simultaneous capacity-and-scheduling optimization, which is appropriate for public or fast-charging systems with stochastic arrival patterns. The present study instead adopts an energy-block representation of daily shuttle charging demand because the RMUTL case is a dedicated

 doi:10.20944/preprints202605.0703.v1

captive-fleet application with fixed routes, predictable overnight parking, and known institutional operating schedules. This modelling choice is appropriate for the present use case, but future work could extend the framework to include intra-day dispatch optimization, V2G operation, and time-varying tariff arbitrage.

Beyond methodology type, the comparison reveals important differences in problem framing. Studies adopting MILP or convex programming [12,13] typically formulate the PV–BESS sizing problem with a unified objective, but cost data and constraint parameters are calibrated to public fast-charging contexts where stochastic arrival patterns dominate. In contrast, the present captive-fleet formulation deliberately treats charging demand as deterministic energy blocks aligned with the academic calendar, allowing the rooftop-area and one-day autonomy constraints to govern the optimum without competing demand-uncertainty constraints. This distinction is not a limitation but a structural feature of institutional fleets, and it is the precise reason the closed-form KKT solution is admissible here while not being so for public-charging studies.

A second methodological distinction concerns the treatment of investment risk. Among the comparison set, only Wei et al. [34] and the present study explicitly quantify stochastic NPV under multi-parameter uncertainty. The 5,000-scenario Monte Carlo simulation conducted here resolves seven joint uncertainty sources—diesel price, fuel escalation, solar resource, fleet utilization, PV electricity-credit value, O&M cost, and discount rate—and reports both $VaR_5\%$ and $CVaR_5\%$. This goes beyond typical sensitivity analyses limited to one or two parameters and provides a defensible downside-risk metric for institutional finance committees that must justify capital commitments under public-sector procurement rules.

Third, the integration of carbon payback alongside financial payback distinguishes this study from purely techno-economic comparisons. Most reviewed studies report annual CO_2 savings but do not normalize against embodied PV–BESS emissions; consequently they cannot speak to the temporal alignment between economic and environmental returns. The present study finds that the carbon payback (0.83 years; 1.07 years including year-10 BESS replacement) is 5.7–7.3 times faster than the financial payback. This insight is institutionally important because sustainability reporting frameworks (e.g., GRI, TCFD, AUN-QA institutional sustainability indicators) increasingly require carbon-payback disclosure independent of financial metrics.

4.4. Limitations

Several limitations should be acknowledged. First, the annual distance and charging-energy estimates were derived from the institutional operating schedule rather than from GPS logs, odometer records, or charger-meter data; therefore, the present study should be interpreted as a planning-level analytical and techno-economic assessment, not as a fully field-validated operational deployment. The optimization result is analytically derived and numerically verified by DE, while future work should validate the demand, charging, and PV-surplus assumptions using measured operational data. The incremental acquisition cost of the electric shuttle vans was based on assumed market prices, with a total premium of USD 171,429 (≈ USD 17,143/vehicle), and should be updated using actual supplier quotations, exchange rates, import conditions, vehicle-registration category, procurement channel, and the applicable EV 3.5 incentive rules at the time of purchase. Because EV 3.5 subsidy eligibility varies by vehicle type, battery capacity, price ceiling, and local-production condition, no direct subsidy was deducted from the base-case cash flow in order to maintain a conservative financial assessment. Second, the LOLE model treats grid availability as a time-stationary Bernoulli process, which is suitable for screening-level reliability assessment but does not capture seasonal outage clustering, monsoon-related faults, or consecutive low-solar days; a Markov-chain extension could reproduce these clustering effects more faithfully. Third, PV degradation was assumed to be 0.5%/yr; higher degradation under tropical conditions may reduce the PV electricity-credit value, although the project economics are driven mainly by avoided diesel fuel and maintenance savings. Fourth, the analysis assumes a constant PV electricity-credit value of USD 0.0629/kWh (2.20 THB/kWh); if this credit were discontinued after year 5, the NPV would decrease

 doi:10.20944/preprints202605.0703.v1

from USD 86,293 to approximately USD 61,048, and even without any PV credit over the project lifetime the NPV would remain positive at approximately USD 38,973. Fifth, BESS round-trip efficiency and depth of discharge were treated as deterministic constants; modelling their gradual decline through cycle-aware battery ageing [40] would increase the required nominal capacity. These limitations indicate the need for field-data validation and updated procurement assumptions, but they do not change the overall conclusion that the EV + PV–BESS transition remains financially and environmentally robust.

In addition, the present analysis does not include charger queueing or scheduling stochasticity. Sequential charging of five vans at one 7.4 kW Level-2 connector requires approximately 10.6 h, which fits within the assumed 12.33 h overnight window with 1.7 h slack. Connector-rotation logistics, operator availability, and the consequence of a single-charger failure (no redundancy) are not modelled and represent operational risks that should be evaluated before deployment.

Furthermore, BESS dispatch is assumed to be naïve overnight charging from PV-stored energy and grid backup; no degradation-aware dispatch, demand-response participation, or vehicle-to-grid (V2G) revenue is included. These omissions are deliberate, given the fixed-route captive nature of the fleet, but they imply that the reported NPV is conservative relative to a fully optimized smart-charging operation.

The Monte Carlo input distributions are based on expert judgment informed by recent regional and international references, rather than on historical time-series fits. The 100% probability of positive NPV across the 5,000-scenario set should therefore be interpreted as conditional on the adopted uncertainty ranges; a stress-scenario analysis is provided in Section 3.6 to test robustness against more adverse joint outcomes.

Embodied-carbon factors for the PV array (600 $kgCO_2/kWp$, after Frischknecht et al. [31]) and the LFP BESS (75 $kgCO_2/kWh$, after Emilsson and Dahllöf [43]) are taken from current IEA-PVPS Task 12 and IVL datasets. These values reflect contemporary manufacturing energy mixes and may evolve as cell-production supply chains decarbonize; the carbon payback period reported here is thus an upper bound under current manufacturing carbon intensity.

Finally, the financial analysis uses a fixed exchange rate of 35 THB/USD. A sensitivity to ±10% movement in the exchange rate (32–38 THB/USD) is provided in Section 3.8 alongside the tornado analysis; this captures the dominant currency exposure in CAPEX (PV modules, BESS cells, inverters) and diesel pricing.

4.5. Implications for Practice and Policy

The proposed framework has several practical and policy implications. For institutional fleet operators—universities, hospitals, government agencies, and corporate campuses with fixed routes and predictable parking—the closed-form active-constraint rule (derived via KKT analysis under monotonicity) provides an immediately deployable sizing heuristic: maximize PV up to the available rooftop area and size BESS only to the required one-day autonomy. This avoids costly oversizing of storage, which is the single most influential CAPEX line item in PV–BESS infrastructure. For Thai institutional decision-makers, the 6.1-year simple payback combined with a 0.83-year carbon payback positions captive-fleet electrification as one of the highest-leverage decarbonization actions accessible to non-grid actors. From a policy perspective, the results suggest that aligning PV–BESS station-sizing standards with the active-constraint logic identified here could simplify permit processes and accelerate institutional EV adoption. The framework is also transferable to ASEAN peers with similar solar resources (PSH ≈ 4.5–5.5 h/day) and academic-calendar fleets, including university shuttles in Vietnam, Indonesia, and the Philippines. Finally, the demonstration that the PV–BESS infrastructure alone has a 2.4-year payback indicates that institutions hesitant to commit to full vehicle replacement may begin with charging-infrastructure deployment for future-ready EV adoption, capturing immediate PV electricity-credit value while preserving optionality for fleet electrification when EV procurement costs decline.

 doi:10.20944/preprints202605.0703.v1

4.6. Transferability and Boundary Conditions of the Closed-Form Sizing Rule

The closed-form rule transfers cleanly to other captive fleets that share four structural features: (i) fixed routes with predictable terminal parking; (ii) overnight charging windows that exceed the single-charger sequential service time; (iii) a hard rooftop-area or solar-resource cap that binds the PV upper bound; and (iv) a daily energy demand that is moderate relative to commercially available BESS module sizes (so commercial rounding does not dominate the design). University fleets, hospital shuttles, government-agency vehicle pools, and corporate-campus shuttles meet these conditions in most cases. The rule is less directly applicable to (a) public fast-charging where arrival patterns are stochastic and demand is not known in advance, (b) multi-shift fleets where overnight windows are short or absent, and (c) fleets with daytime opportunity charging from PV directly, where the BESS autonomy constraint is no longer the binding lower bound. In these cases, the present framework should be replaced by a stochastic dispatch optimization (e.g., MILP capacity-and-scheduling co-optimization).

5. Conclusions

This study developed and numerically verified a closed-form active-constraint sizing framework, derived via Karush–Kuhn–Tucker (KKT) analysis under verified monotonicity of the NPV objective, for siting and sizing hybrid PV–BESS charging infrastructure for a fixed-route institutional electric shuttle fleet. The framework was applied to the RMUTL academic shuttle route between Huay Kaew and Doi Saket campuses, where the fleet operation is defined by fixed routes, predictable terminal parking, and an academic operating calendar.

The main findings are as follows. First, the two-station distributed configuration is economically and operationally preferable to a single centralized station. It eliminates 47,600 km/year of non-revenue dead-run travel, avoids 8,901 kWh/year of unnecessary EV energy consumption, and increases system NPV from USD 36,980 to USD 86,293. This gives a two-station NPV advantage of USD 49,313, confirming that charging-station location is a key determinant of lifecycle performance for captive electric shuttle fleets.

Second, the KKT analysis shows that the optimal sizing is governed by two active constraints: the BESS one-day autonomy constraint and the PV rooftop-area constraint. The resulting closed-form solution gives $P_{PV}^{*} = 30$ kWp and $E_{BESS}^{*} = 94.85$kWh per station. After commercial rounding, the practical system design is 60 kWp PV, 200 kWh LFP BESS, and two 7.4 kW AC chargers. The principal methodological contribution is that the sizing problem is reduced from an iterative numerical search to a transparent engineering rule: maximize PV within the available rooftop area and size the BESS only to the required daily autonomy.

Third, the proposed EV + PV–BESS transition is financially viable under the base-case assumptions. Including both charging infrastructure and the incremental acquisition cost of the electric shuttle vans, the project achieves NPV = USD 86,293, IRR = 12.9%, a simple payback period of 6.1 years, and a discounted payback period of 8.8 years. The total cost of ownership decreases from USD 0.268/km for the diesel baseline to USD 0.231/km for the EV + PV–BESS case, corresponding to a 14.0% reduction in lifecycle transport cost.

Fourth, the environmental benefits are substantial. Annual CO_2 emissions decrease from 64.39 tCO_2/year for the diesel baseline to 2.64 tCO_2/year under the conservative 85% solar-charging assumption. This represents a 95.9% reduction, or approximately 926.3 tCO_2 avoided over the 15-year project lifetime. The initial carbon payback period is 0.83 years, while the adjusted carbon payback period increases to 1.07 years when the year-10 BESS replacement is included in the lifecycle carbon boundary. Both values indicate that the embodied carbon of the PV–BESS infrastructure is recovered well before the financial payback period.

Finally, the Monte Carlo simulation with 5,000 scenarios confirms the robustness of the investment under techno-economic uncertainty. Within the adopted uncertainty ranges, all simulated cases remained NPV-positive, giving $P(NPV > 0) = 100\%$ for the 5,000-scenario set.

 doi:10.20944/preprints202605.0703.v1

Overall, the proposed KKT-based framework provides a practical and transferable method for planning PV–BESS charging infrastructure for institutional fleets with fixed routes and predictable parking locations. The approach is applicable to university, hospital, government, and campus shuttle services in Thailand and similar Southeast Asian contexts. Future research should validate the model using GPS-based operating data, measured charger-energy records, multi-year solar-resource data, and campus outage records. Further extensions should also consider dynamic dispatch, battery ageing, tariff-aware operation, and vehicle-to-grid strategies [41,42].

Author Contributions: Conceptualization, K.S. and T.S.; methodology, K.S. and T.S.; software, K.S.; validation, K.S., T.S. and N.P.; formal analysis, K.S.; investigation, K.S., T.S., J.T., A.N., N.P., M.N., N.K., W.M. and K.N.; resources, T.S.; data curation, K.S.; writing—original draft preparation, K.S. and T.S.; writing—review and editing, T.S.; visualization, K.S.; supervision, T.S.; project administration, T.S.; funding acquisition, T.S. All authors have read and agreed to the published version of the manuscript.

Funding: This research was funded by the Fundamental Fund for fiscal year 2026, project number 4826436.

Data Availability Statement: The data presented in this study are available on request from the corresponding author.

Acknowledgments: The authors acknowledge the internal technical, facility, and equipment support provided by the Clean Energy System Research Unit (CES-RMUTL) and the Division of Electrical Engineering, Faculty of Engineering, Rajamangala University of Technology Lanna, Chiang Mai.

Conflicts of Interest: The authors declare no conflicts of interest. The funder had no role in the design of the study; in the collection, analyses, or interpretation of data; in the writing of the manuscript; or in the decision to publish the results.

Abbreviations

The following abbreviations are used in this manuscript:

BESS	Battery Energy Storage System
CAPEX	Capital Expenditure
COE	Cost of Energy
CPBP	Carbon Payback Period
CVaR	Conditional Value-at-Risk
DOD / DoD	Depth of Discharge
DS	Doi Saket
EV	Electric Vehicle
GEF	Grid Emission Factor
HK	Huay Kaew
ICE	Internal Combustion Engine
IRR	Internal Rate of Return
KKT	Karush–Kuhn–Tucker
LFP	Lithium Iron Phosphate
LOLE	Loss of Load Expectation
NPV	Net Present Value
PSH	Peak Solar Hour
PV	Photovoltaic
RMUTL	Rajamangala University of Technology Lanna
TCO	Total Cost of Ownership
VaR	Value-at-Risk

References

1. IEA. *Global EV Outlook 2024*; International Energy Agency: Paris, France, 2024.

 doi:10.20944/preprints202605.0703.v1

2. IPCC. *Climate Change 2022: Mitigation of Climate Change; Contribution of Working Group III to the Sixth Assessment Report of the Intergovernmental Panel on Climate Change*; Cambridge University Press: Cambridge, UK, 2022. https://doi.org/10.1017/9781009157926.
3. Juang, J.; Williams, W.G.; Ramshankar, A.T.; Schmidt, J.; Xuan, K.; Bozeman, J.F., III. A Multi-Scale Lifecycle and Technoeconomic Framework for Higher Education Fleet Electrification. *Sci. Rep.* **2024**, *14*, 4938. https://doi.org/10.1038/s41598-024-54752-z.
4. Thailand Board of Investment. EV 3.5: Support Measures for the Second Phase of Electric Vehicle Promotion, 2024–2027; Thailand Board of Investment: Bangkok, Thailand, 2024.
5. Thailand Greenhouse Gas Management Organization (TGO). Grid Emission Factor. Available online: http://thaicarbonlabel.tgo.or.th (accessed on 9 October 2025).
6. Sengupta, M.; Xie, Y.; Lopez, A.; Habte, A.; Maclaurin, G.; Shelby, J. The National Solar Radiation Data Base (NSRDB). *Renew. Sustain. Energy Rev.* **2018**, *89*, 51–60. https://doi.org/10.1016/j.rser.2018.03.003.
7. Ngao-det, M.; Thongpron, J.; Namin, A.; Patcharaprakiti, N.; Muangjai, W.; Somsak, T. Systematic Optimize and Cost-Effective Design of a 100% Renewable Microgrid Hybrid System for Sustainable Rural Electrification in Khlong Ruea, Thailand. *Energies* **2025**, *18*, 1628. https://doi.org/10.3390/en18071628.
8. Srasuay, K.; Thongpron, J.; Namin, A.; Nakaiam, K.; Panlawan, N.; Ngaodet, M.; Muangjai, W.; Somsak, T.; Patcharaprakiti, N. A techno-economic analysis of a 48 V mini shuttle electric vehicle with a solar-assisted system for a carbon-neutral green campus. *Jpn. J. Appl. Phys.* **2025**, *64*, 07SP03. https://doi.org/10.35848/1347-4065/addf58.
9. Rodríguez-Molina, J.; Martínez-Núñez, M.; Martínez, J.F.; Pérez-Aguiar, W. Business Models in the Smart Grid: Challenges, Opportunities and Proposals for Prosumer Profitability. *Energies* **2014**, *7*, 6142–6171. https://doi.org/10.3390/en7096142.
10. Lam, A.Y.S.; Leung, Y.-W.; Chu, X. Electric Vehicle Charging Station Placement: Formulation, Complexity, and Solutions. *IEEE Trans. Smart Grid* **2014**, *5*, 2846–2856. https://doi.org/10.1109/TSG.2014.2344684.
11. Awasthi, A.; Venkitusamy, K.; Padmanaban, S.; Selvamuthukumaran, R.; Blaabjerg, F.; Singh, A.K. Optimal Planning of Electric Vehicle Charging Station at the Distribution System Using Meta-Heuristic Technique. *Energy* **2017**, *133*, 70–78. https://doi.org/10.1016/j.energy.2017.05.094.
12. Shareef, H.; Islam, M.M.; Mohamed, A. A Review of the Stage-of-the-Art Charging Technologies, Placement Methodologies, and Impacts of Electric Vehicles. *Renew. Sustain. Energy Rev.* **2016**, *64*, 403–420. https://doi.org/10.1016/j.rser.2016.06.033.
13. Boonprong, S.; Punturasan, N.; Varnakovida, P.; Prechathamwong, W. Towards Sustainable Urban Mobility: Voronoi-Based Spatial Analysis of EV Charging Stations in Bangkok. *Sustainability* **2024**, *16*, 4729. https://doi.org/10.3390/su16114729.
14. Huang, Z.; Fang, B.; Deng, J. Multi-objective optimization strategy for distribution network considering V2G-enabled electric vehicles in building integrated energy system. *Prot. Control Mod. Power Syst.* **2020**, *5*, 7. https://doi.org/10.1186/s41601-020-0154-0.
15. Leone, C.; Fernández-Ramírez, L.M. Multi-Objective Optimization of PV and Energy Storage Systems for Ultra-Fast Charging Stations. *IEEE Access* **2022**, *10*, 14208–14224. https://doi.org/10.1109/ACCESS.2022.3147672.
16. Boyd, S.; Vandenberghe, L. *Convex Optimization*; Cambridge University Press: Cambridge, UK, 2004.
17. Kucevic, D.; Tepe, B.; Englberger, S.; Parlikar, A.; Mühlbauer, M.; Bohlen, O.; Jossen, A.; Hesse, H. Standard Battery Energy Storage System Profiles: Analysis of Various Applications for Stationary Energy Storage Systems Using a Holistic Simulation Framework. J. Energy Storage 2020, 28, 101077.
18. Olabi, A.G.; Abdelkareem, M.A. Renewable Energy and Climate Change. *Renew. Sustain. Energy Rev.* **2022**, *158*, 112111. https://doi.org/10.1016/j.rser.2022.112111.
19. Hannan, M.A.; Hoque, M.M.; Mohamed, A.; Ayob, A. Review of Energy Storage Systems for Electric Vehicle Applications: Issues and Challenges. *Renew. Sustain. Energy Rev.* **2017**, *69*, 771–789. https://doi.org/10.1016/j.rser.2016.11.171.
20. Lipu, M.S.H.; Hannan, M.A.; Hussain, A.; Hoque, M.M.; Ker, P.J.; Saad, M.H.M.; Ayob, A. A Review of State of Health and Remaining Useful Life Estimation Methods for Lithium-Ion Battery in Electric Vehicles:

 doi:10.20944/preprints202605.0703.v1

Challenges and Recommendations. *J. Clean. Prod.* **2018**, *205*, 115–133. https://doi.org/10.1016/j.jclepro.2018.09.065.

21. Storn, R.; Price, K. Differential Evolution—A Simple and Efficient Heuristic for Global Optimization over Continuous Spaces. *J. Glob. Optim.* **1997**, *11*, 341–359. https://doi.org/10.1023/A:1008202821328.
22. Ochoa-Correa, D.; Sempértegui-Moscoso, E.; Villa-Ávila, E.; Arévalo, P.; Espinoza, J.L. PV Solar-Powered Electric Vehicles for Inter-Campus Student Transport and Low CO_2 Emissions: A One-Year Case Study from the University of Cuenca, Ecuador. *Sustainability* **2025**, *17*, 7595. https://doi.org/10.3390/su17177595.
23. Fiori, C.; Ahn, K.; Rakha, H.A. Power-Based Electric Vehicle Energy Consumption Model: Model Development and Validation. *Appl. Energy* **2016**, *168*, 257–268. https://doi.org/10.1016/j.apenergy.2016.01.097.
24. Schmidt, O.; Hawkes, A.; Gambhir, A.; Staffell, I. The Future Cost of Electrical Energy Storage Based on Experience Rates. *Nat. Energy* **2017**, *2*, 17110. https://doi.org/10.1038/nenergy.2017.110.
25. Kebede, A.A.; Coosemans, T.; Messagie, M.; Jemal, T.; Behabtu, H.A.; Van Mierlo, J.; Berecibar, M. Techno-Economic Analysis of Lithium-Ion and Lead–Acid Batteries in Stationary Energy Storage Application. *J. Energy Storage* **2021**, *40*, 102748. https://doi.org/10.1016/j.est.2021.102748.
26. Mongird, K.; Viswanathan, V.; Alam, J.; Vartanian, C.; Sprenkle, V.; Baxter, R. *2020 Grid Energy Storage Technology Cost and Performance Assessment*; Technical Report PNNL-30461; Pacific Northwest National Laboratory: Richland, WA, USA, 2020.
27. Way, R.; Ives, M.C.; Mealy, P.; Farmer, J.D. Empirically Grounded Technology Forecasts and the Energy Transition. *Joule* **2022**, *6*, 2057–2082. https://doi.org/10.1016/j.joule.2022.08.009.
28. Hesse, H.C.; Schimpe, M.; Kucevic, D.; Jossen, A. Lithium-Ion Battery Storage for the Grid—A Review of Stationary Battery Storage System Design Tailored for Applications in Modern Power Grids. *Energies* **2017**, *10*, 2107. https://doi.org/10.3390/en10122107.
29. Lambert, T.; Gilman, P.; Lilienthal, P. Micropower System Modeling with HOMER. In *Integration of Alternative Sources of Energy*; Farret, F.A., Simões, M.G., Eds.; John Wiley & Sons: Hoboken, NJ, USA, 2006; pp. 379–418. https://doi.org/10.1002/0471755621.ch15.
30. Rockafellar, R.T.; Uryasev, S. Optimization of Conditional Value-at-Risk. *J. Risk* **2000**, *2*, 21–41. https://doi.org/10.21314/JOR.2000.038.
31. Frischknecht, R.; Stolz, P.; Krebs, L.; de Wild-Scholten, M.; Sinha, P.; Fthenakis, V.; Kim, H.C.; Raugei, M.; Stucki, M. *Life Cycle Inventories and Life Cycle Assessments of Photovoltaic Systems*; IEA PVPS Task 12, Report T12-19:2020; International Energy Agency Photovoltaic Power Systems Programme: Paris, France, 2020.
32. Tu, R.; Gai, Y.J.; Farooq, B.; Posen, D.; Hatzopoulou, M. Electric Vehicle Charging Optimization to Minimize Marginal Greenhouse Gas Emissions from Power Generation. *Appl. Energy* **2020**, *277*, 115517. https://doi.org/10.1016/j.apenergy.2020.115517.
33. Denholm, P.; Hand, M. Grid Flexibility and Storage Required to Achieve Very High Penetration of Variable Renewable Electricity. *Energy Policy* **2011**, *39*, 1817–1830. https://doi.org/10.1016/j.enpol.2011.01.019.
34. Wei, Y.; Han, T.; Wang, S.; Qin, Y.; Ouyang, M. An Efficient Data-Driven Optimal Sizing Framework for Photovoltaics–Battery-Based Electric Vehicle Charging Microgrid. *J. Energy Storage* **2022**, *55*, 105670. https://doi.org/10.1016/j.est.2022.105670.
35. Sun, C.; Zhao, X.; Qi, B.; Xiao, W.; Zhang, H. Economic and Environmental Analysis of Coupled PV–Energy Storage–Charging Station Considering Location and Scale. *Appl. Energy* **2022**, *328*, 119680. https://doi.org/10.1016/j.apenergy.2022.119680.
36. Dong, X.-J.; Shen, J.-N.; Liu, C.-W.; Ma, Z.-F.; He, Y.-J. Simultaneous Capacity Configuration and Scheduling Optimization of an Integrated Electrical Vehicle Charging Station with Photovoltaic and Battery Energy Storage System. *Energy* **2024**, *289*, 129991. https://doi.org/10.1016/j.energy.2023.129991.
37. Nafeh, A.E.-S.A.; Omran, A.E.-F.A.; Elkholy, A.; Yousef, H.K.M. Optimal Economical Sizing of a PV–Battery Grid-Connected System for Fast Charging Station of Electric Vehicles Using Modified Snake Optimization Algorithm. *Results Eng.* **2024**, *22*, 101965. https://doi.org/10.1016/j.rineng.2024.101965.
38. Gönül, Ö.; Duman, A.C.; Güler, Ö. Multi-Objective Optimal Sizing and Techno-Economic Analysis of On- and Off-Grid Hybrid Renewable Energy Systems for EV Charging Stations. *Sustain. Cities Soc.* **2024**, *114*, 105846. https://doi.org/10.1016/j.scs.2024.105846.

 doi:10.20944/preprints202605.0703.v1

39. Kassem, R.; El-Rifaie, A.M.; Saleeb, H.; et al. Design and Optimal Sizing of PV/Grid-Integrated EV Charging Stations at Universities: A Case Study. *Unconvent. Resour.* **2025**, *8*, 100213. https://doi.org/10.1016/j.uncres.2025.100213.
40. Naumann, M.; Spingler, F.B.; Jossen, A. Analysis and Modeling of Cycle Aging of a Commercial LiFePO4/Graphite Cell. *J. Power Sources* **2020**, *451*, 227666. https://doi.org/10.1016/j.jpowsour.2019.227666.
41. Brinkel, N.B.G.; Schram, W.L.; AlSkaif, T.A.; Lampropoulos, I.; van Sark, W.G.J.H.M. Should We Reinforce the Grid? Cost and Emission Optimization of Electric Vehicle Charging Under Different Transformer Limits. *Appl. Energy* **2020**, *276*, 115285. https://doi.org/10.1016/j.apenergy.2020.115285.
42. Tushar, W.; Yuen, C.; Saha, T.K.; Morstyn, T.; Chapman, A.C.; Alam, M.J.E.; Hanif, S.; Poor, H.V. Peer-to-Peer Energy Systems for Connected Communities: A Review of Recent Advances and Emerging Challenges. *Appl. Energy* **2021**, *282*, 116131. https://doi.org/10.1016/j.apenergy.2020.116131.
43. Emilsson, E.; Dahllöf, L. Lithium-Ion Vehicle Battery Production: Status 2019 on Energy Use, CO_2 Emissions, Use of Metals, Products' Environmental Footprint, and Recycling. IVL Swedish Environmental Research Institute, Report C 444, Stockholm, Sweden, 2019.